(12) INTERNATIONAL APPLICATION PUBLISHED UNDER THE PATENT COOPERATION TREATY (PCT)

(19) World Intellectual Property Organization
International Bureau

(43) International Publication Date
7 November 2002 (07.11.2002)

PCT

(10) International Publication Number
WO 02/087427 A1

(51) International Patent Classification[7]: A61B 3/10, 3/14

(21) International Application Number: PCT/NL02/00290

(22) International Filing Date: 2 May 2002 (02.05.2002)

(25) Filing Language: English

(26) Publication Language: English

(30) Priority Data:
01201594.7 2 May 2001 (02.05.2001) EP
01204459.0 21 November 2001 (21.11.2001) EP

(71) Applicants *(for all designated States except US)*: **UNIVERSITAIR MEDISCH CENTRUM UTRECHT** [NL/NL]; Heidelberglaan 100, NL-3584 CX Utrecht (NL). **UNIVERSITEIT UTRECHT** [NL/NL]; Heidelberglaan 8, NL-3584 CS Utrecht (NL).

(72) Inventors; and

(75) Inventors/Applicants *(for US only)*: **van de KRAATS, Jan** [NL/NL]; Beekweg 10, NL-3881 LH Putten (NL). **BERENDSCHOT, Toussaint, Theresia, Johannes, Maria** [NL/NL]; Witsenburgselaan 43, NL-6524 RE Nijmegen (NL). **ZAGERS, Niels, Petrus, Antonius** [NL/NL]; Gildstraat 97, NL-3572 EL Utrecht (NL).

(74) Agent: **PRINS, A.W.**; c/o Vereenigde, Nieuwe Parklaan 97, NL-2587 BN The Hague (NL).

(81) Designated States *(national)*: AE, AG, AL, AM, AT (utility model), AT, AU, AZ, BA, BB, BG, BR, BY, BZ, CA, CH, CN, CO, CR, CU, CZ (utility model), CZ, DE (utility model), DE, DK (utility model), DK, DM, DZ, EC, EE (utility model), EE, ES, FI (utility model), FI, GB, GD, GE, GH, GM, HR, HU, ID, IL, IN, IS, JP, KE, KG, KP, KR, KZ, LC, LK, LR, LS, LT, LU, LV, MA, MD, MG, MK, MN, MW, MX, MZ, NO, NZ, OM, PH, PL, PT, RO, RU, SD, SE, SG, SI, SK (utility model), SK, SL, TJ, TM, TN, TR, TT, TZ, UA, UG, US, UZ, VN, YU, ZA, ZM, ZW.

(84) Designated States *(regional)*: ARIPO patent (GH, GM, KE, LS, MW, MZ, SD, SL, SZ, TZ, UG, ZM, ZW), Eurasian patent (AM, AZ, BY, KG, KZ, MD, RU, TJ, TM), European patent (AT, BE, CH, CY, DE, DK, ES, FI, FR,

[Continued on next page]

(54) Title: APPARATUS AND METHOD FOR MEASUREMENT OF SPECIFIC CHARACTERISTICS OF EYES

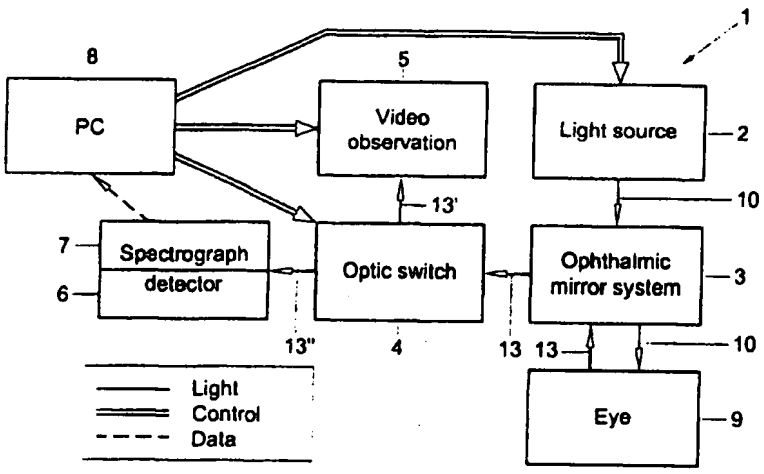

Schematic representation of the apparatus

(57) Abstract: Apparatus for measurements of at least two specific characteristics of eyes, comprising a light source (2), means for (3) transferring light from said light source (2) to an eye (9) and light receptor means (6) for reception of light reflected by said eye (9), wherein said light source (2) comprises means for providing multi-wavelength light, specifically white light, the light receptor means detecting means (6) comprising at least spectrograph means (7) for analysing said light reflected and preferably a video observation means (5).

WO 02/087427 A1

GB, GR, IE, IT, LU, MC, NL, PT, SE, TR). OAPI patent (BF, BJ, CF, CG, CI, CM, GA, GN, GQ, GW, ML, MR, NE, SN, TD, TG).

Published:

— *with international search report*

— *before the expiration of the time limit for amending the claims and to be republished in the event of receipt of amendments*

For two-letter codes and other abbreviations, refer to the "Guidance Notes on Codes and Abbreviations" appearing at the beginning of each regular issue of the PCT Gazette.

APPARATUS AND METHOD FOR MEASUREMENT OF SPECIFIC CHARACTERISTICS OF EYES

The invention relates to an apparatus for measurement of specific characteristics of eyes. Such apparatus is known from US 5873831.

In this known apparatus a laser light source is provided for directing monochromatic light into an eye. A light collecting system is provided for collecting light scattered by the eye, which is then directed to a spectrally highly selective system for separating different types of light. Analysing means are then provided for analysing the light received by said selective means for analyses of macular carotenoid pigment deposition.

This known apparatus has the advantage that it can be used for accurate analysis of macular carotenoid pigment deposition. However, no further characteristics can be measured using the same apparatus. Furthermore, with such apparatus said light has to be directed into said eye steadily for a predetermined, relatively long time. Damage to an eye could occur when used improperly.

An object of the present invention is to provide for an apparatus with which at least two characteristics of an eye can be measured.

A further object of the present invention is to provide for such apparatus using a single light source.

A still further object of the present invention is to provide for such apparatus which enables assessment of at least two of the following three characteristics substantially simultaneously:

- spatial distribution of the fundus reflectance in a pupil plane of an eye;
- the part of the retina used for fixation; and
- the spectral fundus reflectance along a line in the pupil plane.

The present invention further has the object to provide for a method for measurements of specific characteristics of eyes, with which method substantially instantaneously measurement and analyses of at least two characteristics of an eye can be obtained.

These and other objects of the invention are met by providing an apparatus having a light source which provides light of different wave lengths, especially white light, which is directed into an eye and whereby analysing means are provided for analysis of light reflected by said eye. At least spectrographic means are provided for analysing the spectral pattern and/or distribution of the light reflected, wherein analysing means are provided for assessment of fundus reflection in the pupil plane and/or spectral fundus reflectance along a line in the pupil plane and/or measurement of the part of the retina used for fixation.

Preferably substantially white light is transmitted from a light source, from which light red light can be filtered out, whereas the heat of the light can be substantially absorbed. Surprisingly it has been found that light having longer wavelengths may normally be disregarded. Filtering will result in less heating. The remaining light is transferred through a hole in a mirror, from the back side thereof, into an eye, approximately through the centre of the lens system of said eye, accurately focussed by lenses and/or diaphragms. This light is reflected by at least the retina and transmitted back through said lens system, onto the reflecting surface of said mirror, around said hole. Said mirror is preferably angled relative to the direction of the light transferred into said eye, such that it can be transferred to said analysis means. This enables good separation of the going light going into the eye and the less intensive light reflected, which is to be analysed. Interference is substantially obviated.

In a preferred embodiment of the present invention light reflected is directed at will either to a video image system or to a spectrograph, for example by means of an optical switch comprising a movable mirror. Lenses or

polarisation means such as filters can be provided for varying a plane of detection and/or imaging, especially between the optical switch and the video image system.

Computer means comprising analysing software can be provided for processing digital images of the reflected light, which images can be obtained by for example a CCD-camera, a digital video system or the like. By digitising the images obtained, such as light reflection images and spectrographs accurate analyses can be obtained almost instantaneously by said computer means.

Various advantageous embodiments of an apparatus and method according to the present invention are presented in the appending claims. By way of example an advantageous embodiment will be described, with reference to the drawings. These show:

fig. 1 schematically an apparatus according to the present invention;

fig. 2 schematically a light source of an apparatus according to fig. 1;

fig. 3 schematically a ophthalmic mirror system of an apparatus according to fig. 1;

fig. 4 schematically an optical switch of an apparatus according to fig. 1;

fig. 5 schematically a video observation system of an apparatus according to fig. 1;

fig. 6 schematically a spectrograph and detector of an apparatus according to fig. 1;

fig. 7 an experimental set-up combining apparatus of fig. 2-6;

fig. 8 an example of a two dimensional dataset;

fig. 9 a diagram showing the relation between reflectance and position in the pupil plane at different wavelengths;

fig. 10 a diagram showing percentage reflectance versus wavelength;

fig. 11 schematically the layout of the experimental apparatus, similar to fig. 1 and the pupil plane and retinal plane configuration; and

fig. 12-15 test results obtained with the apparatus according to fig. 11.

In the drawing the same or corresponding parts have identical or similar reference signs.

Fig. 1 shows schematically an apparatus according to the present invention. The different components will in further detail be described with reference to fig. 2 - 6.

An apparatus 1 according to the present invention, for analysis of characteristics of an eye, comprises a light source 2, an ophthalmic mirror system 3, an optical switch 4, a video observation unit 5, a detector 6 with a spectrograph 7 connected thereto and a computer 8 comprising appropriate software and a monitor. The light source 2 designed such that it emits light of different, multiple wave lengths, especially substantially white light. The light emitted from the light source 2 is focused and passed through said ophthalmic mirror system 3, into an eye 9. The beam 10 of light is emitted into substantially the centre of the lens system of the eye 9, as indicated schematically in fig. 1A, such that it passes substantially straight through a central part 11 of the pupil. Said light is then reflected by inter alia said retina, partly out of said eye 9 through the part 12 of the lens system of the eye surrounding said central part 11. The light reflected, indicated by numerous arrows 13, has a substantially lower intensity then the beam 10 and is somewhat scattered due to the reflection and the reflecting surfaces such as the retina and other surfaces inside the eye. Also contamination of the lens system can influence scattering.

The reflected light 13 is deflected by the ophthalmic mirror system 3 towards the light switch 4. In this light switch the reflected light is either deflected to the video observation unit 5 or to the detector 6 and connected spectrograph 7, for analysing the spatial distribution of the fundus reflection, preferably in the pupil plan, preferably simultaneously, assessment of the part of the retina used for fixation and spectral fundus reflectance along a line in

the pupil plane respectively. The video images and spectrographic images, which are preferably digitised, are fed into the computer unit 8 for processing and viewing said images and the analysing results on the screen.

At least the light source 2, the optical switch, the video observation system 5 and the detector and spectrograph 6, 7 are controlled by the computer unit, which is also used for absloute spectrographic calibration of the apparatus, which is necessary for accurate analysis of the images and spectrographic plots obtained.

Fig. 2 schematically shows a light source 2, from which a controlled beam 10 of light is produced. The actual source of light 14 is the rectangular shaped coil of a 30 W halogen lamp. The top lens system 15 consists of two lenses 16. They image the coil on a diaphragm (not shown), which is optically conjugate with the pupil plane of the investigated eye 9. The diaphragm determines the size of the entrance in the lens system of the eye 9. Between the two relay lenses a set of filters absorbing heat and red light can be placed (not shown) for filtering out substantially all red light and/or heat in said beam 10.

The bottom lens system 17 again consists of a pair of lenses 18. They are drawn as a single lens. In reality, they are preferably spaced a few cm apart. A plane optically conjugate with the retinal plane of the investigated eye 9 is available in between these two lenses. In this plane a diaphragm (not shown) is placed to control the size of the illuminated region on the retina. The light is focused towards the ophthalmic mirror system 3, as shown in fig. 3 by converting lines 10A, crossing in point F.

Fig. 3 shows schematically the ophthalmic mirror system 3 which allows separating the dim light 13 reflected by the eye 9 from the intense beam 10 entering it. The key element is a mirror 19 with a central hole 20 placed optically conjugate with the pupil plane. An image of the coil (beam 10) is focused in the centre of the hole 20 by the light source 2. This image is relayed with a single, aspheric ophthalmic lens 21 to the pupil plane. Because

the rays (schematically shown as lines 10B) are focused substantially within the centre 11 of the eye's lens-system 9A, the rays 10B will continue in their original direction towards the retina. This way, a relatively small spot is illuminated on the retina.

Light 13 reflected from the retina can be considers as a new, small source of light. When the eye 9 is unaccommodated, the lens system 9A of the eye 9 will image the retina in a plane placed at infinity. For light 10 entering the eye 9, only a small part 11 of the eye's pupil was used. The remaining part 12 of the pupil can be used to collect light 13 reflected from the retina. A plane optically conjugate to the retina (not specifically shown) is located in between the ophthalmic lens 21 and the mirror 19 with central hole 20, one focal length behind the ophthalmic lens 21. Both this retinal plane and the largest part of the pupil plane are available via the mirror 19.

The optic switch 4 as schematically shown in fig. 4 comprises three lenses 22, 23 and 24 respectively, and a moveable mirror 25. The mirror 25 is pivotally connected to an axis 26 and is movable between a position "in place" as shown in fig. 4, enclosing an angle of approximately 45 degrees with the main direction of the light 13 (which is in the drawing substantially perpendicular to the centre of lens 22) and a pivoted position out of reach of said light 13. With the mirror 25 "in place", the light 13 is reflected 'upwards' and the right 22 and top lens 23 act as a relay pair (upward, right and left as seen in fig. 4; these can normally be in any desired position). In this case, the light 13 is directed towards a video observation channel of the video observation unit 5, as shown in fig. 5. The mirror 25 can be removed from the beam 13 fast, which makes the light available for the detector 6 and spectrograph 7. In this mode the right 22 and left lens 24 act as a relay pair.

Fig. 5 schematically shows Video observation unit 5. The bottom lens 23 in Figure 5 corresponds to the top lens 23 in Figure 4. The bottom lens 23 relays both the pupil and retinal plane (only two pupil plane rays are drawn). Both planes are available for imaging on the video camera (V). The top

lens system 27 contains an insertable lens 28 (not shown specifically). By removing or inserting this lens 28, the imaged plane is selected. Video images obtained can be displayed on a monitor 29.

Fig. 6 schematically shows a detector 6 and spectrograph 7. The right lens 24 in Figure 6 corresponds to the left lens 24 in Figure 4. This lens 24 images the pupil plane at infinity. A plane optically conjugate to the retina (not specifically shown) is located between this lens 24 and the lens 30 nearest to it at the left, as seen in fig. 6. In this plane a diaphragm is used to limit the observed region of the retina to just within the illuminated region (fig. 1A). The second lens 30 focuses the light on the entrance slit 31 of an imaging spectrograph 7. This slit 31 is in a plane optically conjugate to the pupil plane. The first lens 33 of the spectrograph 7 turns the beam 13D parallel again. The beam 13E traverses a direct vision prism which spectrally decomposes the beam 13E. The light reflected from the eye is divided in light of different wavelengths by said prism, for further analysis. The further lens 34 images the spectrum on a cooled CCD camera 35. The CCD 35 is controlled an read with the computer unit 8.

An Example of an apparatus and method according to the invention is discussed below, with reference to fig. 7-10.

A schematic representation of the set up as seen from above is depicted in Fig. 7. Retinal and pupil planes are indicated with R and P, conjugate planes with R' and P'. At the top right, the optical path starts with a lamp 14. The lenses L1...L4 and the ophthalmic front-lens Lf define the entrance beam, which illuminates a small spot on the retina. Light reflected from the eye is captured by Lf. Separation of the reflected light from the entrance beam is achieved with an ophthalmic mirror Mh 19. The reflected light is either available for observation with a video camera V, or for analysis with an imaging spectrograph. The mode used depends on the position of an insertable mirror Mi 25. The spectrograph image is captured with a cooled integrating CCD camera. Below a more detailed description is given.

The entrance beam is a Maxwellian view system, used for controlled illumination of a small spot on the retina. The light source is a 30 W halogen lamp. An image of the coil of the lamp is relayed in the pupil plane with lens systems L1 and L2, L3 and L4, and the ophthalmic front lens Lf. An aperture placed conjugate to the pupil plane in plane P' after L2 controls the size of the entrance beam in the pupil plane to 1 x 1.5 mm. A cross-wire for fixation is placed in plane R' close to the lamp. In between L1 and L2 the beam is substantially parallel. At this location spectral filters (Fi) are placed, with the purpose to increase the ratio of blue over red light. Eye reflectance is far lower in the blue wavelength region than in the red. In between L3 and L4 the beam is also parallel. A retinal conjugate plane R' is available here, where an aperture controls the angle of the illuminated field on the retina. A 3 degrees field is used for measurements. For alignment, the field angle can be increased to for example 10 degrees.

Light reflected from the eye is very dim compared to the bright entrance beam. Separating both beams is achieved with an ophthalmic mirror Mh 19. The entrance beam passes through the central hole 20 of the mirror. Light reflected from the eye is captured by the remaining part of the mirror. This configuration allows observation of most of the pupil. When the entrance beam is correctly focussed in the pupil plane, reflections at the first surface of the eye (cornea reflections) largely fall in the central hole of mirror. Lens Lf is placed slightly out of center and is slightly tilted, to redirect reflections at the front and back glass-air interfaces out of the center of the beam. Remaining stray-light is accounted for in the dark calibration. For an emmetropic eye, the retina is imaged at infinity by the eye's lens. Lens Lf images the retinal plane in its focal plane, in between Lf and Mh. Mh is conjugate with the pupil plane. Both planes are relayed to either a video observation channel (up-wards), or an imaging spectrograph (left-wards), depending on the position of the insertable mirror Mi 25.

For alignment of the subject a video observation channel is available. When the mirror Mi is flipped in, lenses L5 and L10 act together as a relay pair. Both retinal and pupil plane are relayed to between lens L10 and L11. An insertable lens Li controls which plane is focussed on the video camera chip V. Imaging the retinal plane allows observing whether the subject fixates correctly on the entrance beam. Imaging of the pupil enables observing the location of the entrance beam within the pupil, and is also used to achieve a good focus of the entrance beam in the pupil plane.

When the mirror Mi is removed from the beam, light is available for the imaging spectrograph. Lenses L5 and L6 combined image the pupil plane at infinity. In between L6 and L7 a retinal plane R' is available, where an aperture controls the size of the sampled region on the retina to approximately 2 degrees. An adjustable slit is placed in the focal plane of lens L7. The slit defines a horizontal, bar shaped exit pupil, which measures 1 x 12 mm in the pupil plane of the eye. The slit is in the focal plane of lens L8, which images it at infinity. The light traverses a direct vision dispersion prism (Prism, Linos, Part No. 33 1120). The spectral image is focussed on the chip of a cooled CCD camera (CCD, SBIG, ST-237). The camera is read out in 3x3 binning mode. The spectral image contains 213 points in spectral direction and about 85 points in spatial direction.

It will be clear that the example given above is merely shown for a better understanding of the invention and should in no way be considered as limiting the scope of the invention.

Fig. 8-10 show data obtained with an apparatus and a method according to the present invention.

Fig. 8 shows an example of a two-dimensional data-set: percentage reflectance versus wavelength and position in the pupil plane. The data was binned to 5 nm bandwidth in the spectral direction. The common spectral shape of fundus reflectance is recognizable at the borders of the spectrum. As a

guide to the eye , a single spatial profile at 525 nm is indicated with the fat line.

Fig. 9 shows reflectance versus position in the pupil plane at four different wavelengths. The data is subset of the data shown in fig. 8. The spatial intersections were taken near a number of common laser wavelengths. Data was binned to 5 nm bandwidth before the profiles were obtained. The solid lines are fits of a Gaussian curve of the data.

Fig. 10 shows a percentage reflectance versus wavelength. The data is a subset of the data shown in figure 8. The spectral intersection was taken where the spatial intersections show a maximum. The solid line is a model fit to the data.

An apparatus according to the present invention can be used for example for measurement of both the spatial distribution of the fundus reflectance in the pupil plane and the spectral distribution of the reflectance along a line in the pupil plane. In addition the part of the retina used for fixation should preferably be monitored, to avoid problems because of possible peripheral fixation. The measurements can be made fast and easy resulting in high performance and low cost of the apparatus. The Foveal Reflection Ophthalmoscope according to the present invention will allow study a substantial number of patients in diseases such as age-related macular degeneration and glaucoma, which both ask for a better understanding of their pathogenesis. Since with the Foveal Reflection Ophthalmoscope different parameters can be measured simultaneously (Stiles-Crawford parameters, pigment densities), it will be suited to further knowledge of the pathogeneses.

An apparatus 1 according to the present invention is especially suitable for screening device for photoreceptor densitometry and as a tool for detection of macular and melanin pigment density. Age-related macular degeneration (AMD) is the most common cause of blindness in the Western world. Macular- and melanin pigment possibly protect against AMD. It is

therefore of great importance to have a simple device that can measure these pigments, both for screening and follow-up in case of dietary supplementation.

Furthermore an apparatus according to the present invention is especially but not exclusively suitable as a screening device for densitometry. The presently known technique of densitometry is time consuming and can only be applied at a very limited number of laboratories in the world. Therefore, it is of great importance to have a simple screening device, that provides similar information, which is provided for by the present invention.

In further elucidation of the present invention an experimental apparatus is described, together with test results obtained therewith, in the description hereafter.

The apparatus was basically set up as follows:

A. Overview

A schematic representation of the experimental set up is depicted in Fig. 11A. Retinal and pupil planes are indicated with R and P, conjugate planes with R' and P'. In some cases, adjacent elements or planes are drawn as a single line. At the top right, the entrance beam emerges from a lamp, and passes the lenses L1 through L4 and the ophthalmic front-lens Lf. The entrance beam defines a small entrance pupil in pupil plane P, and illuminates a small spot in the retinal plane R. Light reflected from the eye is captured by lens Lf. Separation of the reflected light from the entrance beam is achieved with an ophthalmic mirror Mh. The reflected light is either available for observation with a video camera V, or for analysis with an imaging spectrograph. The mode used depends on the position of an insertable mirror Mi. The spectrograph image is captured with a cooled integrating CCD camera.

The retinal and pupil plane configuration is depicted in Fig. 11B. In the retinal plane, the illuminated field measures 2.8 degrees. The sampled field is concentric, and measures 1.9 degrees. This overlap assures a complete illumination of the sampled field, despite small errors in focus and aberrations in the optics of the eye. The cross-wire is centered on the illuminated field. In the pupil plane, the entrance pupil is placed centered with, and below the bar shaped exit pupil. Their separation is 0.7 mm. The bar is defined by the slit of the spectrograph. To avoid confusion: the terms entrance and exit are defined with respect to the eye, not the spectrograph.

B. Entrance Beam

The entrance beam forms a Maxwellian view system, used for controlled illumination of a small spot on the retina. An image of the coil of the 30 W halogen lamp is relayed to the pupil plane with achromatic pairs L1, L2 and L3, L4, and the ophthalmic front-lens Lf (20 D, Nikon). The front-lens can be moved in the direction of the beam (z-direction) to focus on the retina. Eye reflectance is far lower in the blue wavelength region than in the red. In the parallel beam between L1 and L2, glass filters F are placed (FG3 and BG38, 3 mm both, Schott), with the purpose of increasing the ratio of blue over red light, and to block most of the infrared light. The intensity of the light entering the eye is 1.10×10^6 Td. An aperture in plane P' after L2 controls the size of the entrance beam in the pupil plane to 0.8×1.2 mm (with the front-lens focussed at infinity). A cross-wire for fixation is placed in plane R' close to the lamp. Between L3 and L4 the beam is again parallel. Another retinal conjugate plane R' is available here, where an aperture controls the visual angle of the illuminated field on the retina. A 2.8 degrees field is used for measurements. For alignment, the field angle is increased to 16 degrees. An additional green filter (VG9, Spindler & Hoyer) is then inserted, to increase contrast of the view. The intensity of the alignment beam is 3.35×10^5 Td.

C. Capturing Light Reflected from the Eye

Light reflected from the eye is captured by lens Lf. The retinal plane is imaged in the focal plane of Lf, the pupil plane in the plane of Mh. Light reflected from the eye is very dim compared to the bright entrance beam. To avoid reflections from the cornea, the entrance and exit light are separated with an ophthalmic mirror Mh conjugate to the pupil plane. When the entrance beam, which passes through the central hole of Mh, is correctly focussed in the pupil plane, reflections from the cornea largely disappear in the same hole. Light reflected from the eye is captured by the remaining part of the mirror. This configuration allows observation of the entire pupil, except for the part covered by the hole. Lens Lf is placed slightly out of center and is slightly tilted, to redirect reflections at the front and back glass-air interfaces out of the center of the beam. This way, the reflections are blocked by the retinal aperture at R' in the spectrograph, and by a small mask on a glass plate in front of L10 in the observation beam.

D. Video Observation of the Retina or Pupil

For alignment of the subject a video observation channel is available. When the mirror Mi is inserted, lenses L5 and L10 act together as a relay pair. Both retinal and pupil plane are relayed to between lens L10 and L11. Lens Li, moved in or out of the beam with a magnetic solenoid, controls which plane is focussed on the video camera chip V (VCB-3512P, Sanyo). Imaging the retina allows focussing of the cross-wire, and observing whether the subject fixates correctly. Imaging of the pupil enables observing the location of the entrance beam within the pupil, and is also used to achieve an optimal focus of the entrance beam in the pupil plane.

E. Imaging Spectrograph

When the mirror Mi is removed from the beam, light is available for the imaging spectrograph. Lenses L5 and L6 combined, image the pupil plane at infinity. In between L6 and L7 a retinal plane R' is available, where an aperture controls the size of the sampled region on the retina to 1.9 degrees. A slit, 0.90 mm wide, is placed in the focal plane of lens L7, conjugate to the pupil plane. The slit defines a horizontal bar shaped exit pupil, which measures 0.8 × 12 mm in the pupil plane of the eye (with the front-lens focussed at infinity). The slit is in the focal plane of lens L8, which images it at infinity. The light traverses a direct vision dispersion prism (Prism, Spindler & Hoyer, Part No. 331120). The spectral image is focussed on the chip of a cooled CCD camera (CCD, ST-237, SBIG). The camera is read out in 3 × 3 binning mode. The spectral image contains 213 points in spectral direction and 85 points in spatial direction.

The following methods were used.

A. Calibration Frames

Reflectance was routinely calibrated with a surface painted with Eastman 6080 white mounted at the end of a black, anodized tube.[2] This painted surface was calibrated against a freshly pressed $BaSO_4$ surface, which we considered the gold standard. The white reference was placed at 445 mm behind the pupil plane and illuminated with the measuring light. Front-lens focus was adjusted to place the reference in a retinal conjugate plane. White reference frames calibrate the spectral output of the lamp, transmission of the optics, sensitivity of the CCD camera, as well as sensitivity variations among CCD camera pixels. To account for stray light in the apparatus and dark current in the CCD camera, reference frames of a dark cloth held at about one meter behind the pupil plane were taken. The integration time of the dark frames matched the integration time of the measured spectrum and the white reference frame.

White and dark reference frames were obtained prior to each session. In case a refractive correction was required during the session, additional dark frames for the new position of the front-lens were obtained at the end of the session.

B. Calculation of Reflectance

Each 3 × 3 binned pixel on the CCD is a detective element, measuring counts at a certain wavelength λ within range Δλ, and at a certain pixel position x in the spatial direction. In this section, an expression for calculating reflectance $R(\lambda, x)$ from the number of counts in the measurement $C_M(\lambda, x)$, the white reference $C_W(\lambda, x)$, and matching dark references $C_{MD}(\lambda, x)$ and $C_{WD}(\lambda, x)$ is derived. $R(\lambda, x)$ is an equivalent reflectance: all sources contributing to the reflected light are considered as if they were diffuse reflectors.[2,13,15] Let $Ph(\lambda)$ be the number of photons per second in the entrance beam, at wavelength λ within range Δλ, either entering the eye or falling on the white-reference surface. Part of the photons will be reflected and back scattered, forming a source of photons in the retinal plane. The number of counts in a pixel is proportional to the photon flux through its detection area and the integration time. The flux through the area A_P spanned by the detective element in the pupil plane at distance d from the retinal plane, is proportional to A_P / d^2. In the measurement situation, the number of detected counts is given by:

$$C_M(\lambda, x) = R(\lambda, x)\, \gamma\, Ph(\lambda)\, t_M\, A_M\, S(\lambda, x) / (2\pi d_{eye}^2) + C_{MD}(\lambda, x), \qquad (1)$$

with t_M the integration time of the measurement, A_M the detection area in the pupil plane, and d_{eye} the axial length of the eye. The constant γ is the ratio of the sampled and illuminated area in the retinal plane. $S(\lambda, x)$ is a sensitivity factor containing transmission of the optics, quantum efficiency and gain of the CCD pixels. The factor 2π accounts for light being reflected into half a sphere. In case of the $BaSO_4$ white reference surface, 99 % of light in the range

400–800 nm is reflected perfectly diffuse or isotropic into a half sphere.[30] A relation similar to Eq. (1) holds for the white reference images:

$$C_W(\lambda, x) = 0.99\,\gamma\,Ph(\lambda)\,t_W\,A_W\,S(\lambda, x) / (2\pi d_{ref}^2) + C_{WD}(\lambda, x), \qquad (2)$$

with t_W the integration time, A_W the detection area in the pupil plane, and d_{ref} the distance between the white reference and the pupil plane. Combining Eq. (1) and (2), the percentage equivalent reflectance is given by:

$$R(\lambda, x) = 0.99\,(t_W / t_M)\,(d_{eye} / d_{ref})^2\,(A_W / A_M) \times$$

$$\{[C_M(\lambda, x) - C_{DM}(\lambda, x)] / [C_W(\lambda, x) - C_{DW}(\lambda, x)]\}. \qquad (3)$$

The factor A_W / A_M, which accounts for changes in scale of the pupil plane with the front-lens position, is calculated from pixel scale S_{PIX} as $(S_{PIX,W} / S_{PIX,M})^2$ (for calibration of S_{PIX}, see Section 3C). The axial length of the eye d_{eye} is calculated from the front-lens focal adjustment. It is assumed that the cornea and eye-lens can be treated as a single flat lens with focal distance 22.29 mm,[30] and that all ametropia can be attributed to variation in axial length of the eye.

An estimation of the error in the reflectance value starts with calculation of the error in the raw pixel data:

$$\sigma = [RN^2 + (N - B) / 3]^{1/2}, \qquad (4)$$

with RN the read-noise of the camera in counts, N the number of counts read from the pixel, and B the bias level of the camera in counts. Typical values are RN = 12, N in the range 150 to 5000, and B = 100. The factor 3 accounts for

3 × 3 on-chip binning. Using the appropriate error propagation mathematics and Eq. (3), an error is attributed to the reflectance.

C. Spectral and Spatial Calibration

For spectral calibration of the spectrograph, images of a mercury lamp illuminating the wall opposing the set-up were obtained. Pixel positions of 7 lines were determined (wavelengths in air: 435.8, 491.6, 546.1, (577.0 + 579.1) / 2, 623.4, 690.8, and 772.9 nm).[31] The wavelength range covered by the spectrograph was 420–790 nm. Dispersion strongly depended on wavelength. At 420 nm the spectral range covered by one 3 × 3 binned pixel was about 0.4 nm; at 760 nm it was about 6 nm. For calibration of pixel scale S_{PIX}, a transparent film containing periodic vertical dark bars was placed in the pupil plane. Images of the wall opposing the set-up revealed the periodic pattern, which enabled scaling of the pupil plane to CCD pixels. Scale was calibrated for the complete range of front-lens settings. With the front-lens focussed at infinity, one 3 × 3 binned pixel corresponded to 0.14 mm in the pupil plane. Prior to the calculation of reflectance, the images were binned and interpolated to 5 nm spectral and 0.1 mm spatial resolution, to correct for the non-linear dispersion of the prism and variable scaling of the pupil plane.

D. Protocol

The research followed the tenets of the Declaration of Helsinki and was approved by the local Medical Ethics Committee. The purpose was explained at the beginning of the experiment, and written informed consent was obtained. The pupil of one eye was dilated with one or two drops tropicamide 0.5 %. A chin-rest and temple-pads, connected to a head-rest, were used to maintain head position. The head-rest can be adjusted in 3 dimensions. This allowed focussing on the pupil plane, and positioning of the entrance beam within the pupil. Subjects were instructed to fixate the cross-wire at all times.

For adjustment of the head-rest the large field with an additional green filter was used. With the large field the pupil lit up more brightly, focus in the pupil plane was more critical, and a larger part of the retina could be seen. The entrance beam was focused in the pupil plane. Care was taken to avoid reflections from the corneal surface of the eye. Fixation was checked in the retinal image. If required, the front-lens focus was adjusted. During focal adjustment the head-rest was moved as well, to maintain a good focus in the pupil plane.

Hereafter, the maximum in the directional reflectance (e.g., the maximum of the Stiles–Crawford effect) was searched for, using the measuring field. During the search, continuously spatial profiles near 540 nm were read from the CCD while discarding the remaining part of the data, thereby achieving a short readout time. Integration time was reduced to 0.25 seconds. At 540 nm the directional reflectance shows up prominently. In the horizontal direction in the pupil plane (along the spectrograph slit) the maximum position is readily observed in a profile plot on a computer display. The maximum in vertical direction was found by a manual search. While scanning vertically, the latest profile was compared by eye to the highest profile till then. The search typically took about 2 minutes. In this period, visual pigments are bleached away for about 97 %.[30] At the optimal entrance position 5 spectra were obtained. Prior to each measurement, subjects were instructed to blink once, keep their eyes wide open, and fixate the cross-wire. Integration time was 1.0 sec. The entire procedure described above, apart from focussing the cross-wire on the retina, was repeated 5 times to test repeatability. Settings of the head-rest were changed on purpose in-between two runs to increase independence.

E. Subjects

All subjects (n = 21) were Caucasian, unfamiliar with any eye disease, and had no complaints on visual acuity. The majority (n = 15, 12 females) fell in the age

group 18–27, mean 22. Six subjects (all male) were aged 40–74. The six older subjects can be considered experienced observers, while the younger subjects were all naïve subjects. Fourteen subjects had no refractive correction. For the other cases, refraction was in the range -1.5 to -4 D, except two older subjects having -6 and -7 D.

With the apparatus and methods described here above the following results were obtained.

A. Reflectance Spectrum Image

An example of an image of two-dimensional reflectance is presented in Fig. 12 (female subject, age 20). The image shows equivalent reflectance of the fovea, expressed as a percentage on a logarithmic scale, versus wavelength and location in the pupil plane. Temporal (T) and nasal (N) side are indicated. The image can be looked upon in two ways: first, as spectral reflectance versus location in the pupil plane, and second, as an optical Stiles–Crawford profile versus wavelength.

Adopting the first view, the characteristics of spectral fundus reflectance are recognized: a decrease towards short wavelengths, with steeper decrements at 590 nm, 510 nm, and at the lowest recorded wavelengths.[2,13,15,32] At the longest wavelengths, ocular pigments, except melanin, are fairly transparent. Below 590 nm, light is efficiently absorbed by blood. The contribution to reflectance from deeper, blood rich layers diminishes, causing the first decrement. Reflectance below 590 nm mainly originates from the receptor cell layer.[2] The second decrement at 510 nm is due to macular pigment. The latter also causes a shallow dip near 460 nm. Absorption by the crystalline lens causes a decline at the shortest recorded wavelengths.

The optical SCE is best observed in the region 510–590 nm. The profile near 540 nm, indicated by the thick line in Fig. 2, presents a typical example. Reflectance shows a bell-shaped dependence on position in the pupil plane, with a maximum slightly on the nasal side of the pupil center.[21,23,25-27] At longer wavelengths, the directional part of the reflectance dissolves in the much larger non-directional part. At shorter wavelengths, absorption by the macular pigment and the crystalline lens leave the bell-shape intact, but strongly reduce the amplitude of the directional reflectance.

B. Spectral Intersections

For each measurement, the spectrum at the pupil position with the highest reflectance at 540 nm was selected (e.g., the spectrum indicated with a thick line in Fig. 2). The spectra were fitted with the van de Kraats *et al.* fundus reflectance model using a least squares method.[2,33] Each data point was assigned a weight one over its error squared. The model describes radiation transfer in the eye with a limited number of reflecting, absorbing, and scattering layers. Spectral properties of the absorbers are taken from the literature. Eight parameters were optimized: reflectance from discs in the outer segments of the photoreceptors R_{disc}, at the inner limiting membrane R_{ilm}, and at the cornea R_{cornea}, the optical densities of melanin D_{mela}, macular pigment D_{mac}, and the aging component of the lens $D_{lens\text{-}a}$, the thickness of the blood layer Th_{blood}, and a parameter accounting for scattering in the choroid D_{scat}. The parameter R_{cornea} was added to the model. Visual pigment density was assumed zero, Stiles–Crawford parameter SC was set at unity. Values for other fixed parameters and a detailed description of the model are given in the original paper.[2]

A sample (n = 5) of spectral reflectance curves spanning the full age range is shown in Fig. 13A. The solid lines represent model fits. The effect of increasing lens absorption with age is apparent from the downward trend with age of the

spectra below 500 nm. Deviations between the data and the model are largest below 425 nm. Here, both reflectance and the power of the entrance beam are low, resulting in a low signal to noise ratio. The mean of all spectra ($n = 5 \times 5 \times 21$) is depicted with a solid line in Fig. 13B, together with data from the literature (squares: Delori and Pflibsen,[15] circles: van de Kraats *et al.*[2]) The mean data are also presented in Table 1, together with relative standard deviation, i.e., the standard deviation of the subject means divided by the mean of subject means. Also given is the relative error, which was first calculated for each subject from the mean of the estimated measurement errors and mean of 25 spectra, and then averaged over subjects.

Table 2A gives a summary of the results of the spectral model fit. The parameter mean PM is the mean of 21 within subject mean values. The standard deviation σ_N is the standard deviation of the subject means with respect to PM. P_{MIN} and P_{MAX} are the lowest and highest within subject means. In some cases P_{MIN} reached zero. This was the lower limit set in the fit algorithm. Apart from estimations for the best fit, the Levenberg–Marquardt method returned 68 % confidence intervals for the fitted parameters.[33] The mean of 21 within subject mean confidence interval estimations CI, is also shown in Table 2A. The study design of 5 measurement series with 5 replacements allowed an estimation of (1) the total standard deviation σ_T, (2) standard deviation with respect to the mean of series σ_S, and (3) the standard deviation of the mean of series σ_M. The coefficient of repeatability CR is defined as the 95% range for the difference in two repeat measurements.[34] The coefficients followed from the mean values of σ_T, σ_S, and σ_M after multiplication by $2\sqrt{2}$.

Fig. 14 gives an impression of the model predictions for single measurements. Fig. 14A shows twenty-five macular pigment density (D_{mac}) estimates for all twenty-one subjects. D_{mac} is known to vary substantially between subjects. The

within subject variability is occasionally large. Six subjects had experience in this type of experiments (1, 3, 12, 13, 17, and 21). They generally showed low variability. In some of the other subjects variability was equally low (e.g., 2, 10 and 11). Others, however, show a large variability (e.g., 9 and 19). Fig. 14B is a similar scatter plot for melanin density (D_{mela}). For melanin, within-subject variation is much smaller compared to D_{mac}. The stability of the melanin data indicates that the high D_{mac} variability is not related to instrumental errors or head instability of the subject. A probable explanation is given in the discussion.

C. Spatial Intersections: SCE Profiles

For each measurement, the profile at 540 nm was selected and fitted with:

$$R(x) = B + A\,10^{-\rho\,(x-xc)^2}, \qquad (5)$$

with R the percentage reflectance, x the location in the pupil plane in mm, B the non-directional background reflectance, A the amplitude of the directional reflectance, ρ a measure for the peakedness, and x_C the center position.[25-27] The fit used a least squares method with each data point assigned a weight one over its error squared.[33] Data included in the fit met two conditions: Distance to either of the pupil edges more than 1 mm, and distance to the entrance beam less than 3 mm.

Optical Stiles–Crawford effect profiles at 540 nm (n = 5) are shown in Fig. 15 for the same subjects as in Fig. 13A. The solid lines represent fits with Eq. (5). At the pupil edges, the profiles drop to zero. The edge of the pupil may span numerous pixels when the bar is far below or above the pupil center, since the vertical width of the bar is much larger than the horizontal width of the pixels. As usual, the maxima show up near the pupil center, with a tendency to the

nasal side.[25-27] Table 2B gives a summary of the SCE parameter fit results (c.f., explanation in Section 4B).

From these results the following can be understood.

A. General Discussion

By the method according to the present invention the feasibility of simultaneous measurement of spectral and directional fundus reflectance has been demonstrated. Both aspects have hitherto been studied separately.[2,13,15,18,19,21-27,32] The course of the spectra and directional aspects agree with earlier results. In the model by van de Kraats *et al.* differences between spectra obtained at the maximum of the optical Stiles–Crawford effect and 2 mm nasally were fitted with a single parameter SC.[2] The model lacks a quantitative relation between SC and position in the pupil plane. Furthermore, the model assumes simultaneous scanning of the entrance and exit pupil. In contrast, we aligned the entrance pupil with the maximum of the Stiles–Crawford effect, and obtained spectra for a range of exit pupil positions. Thus, the van de Kraats *et al.* model as it is, cannot be applied to entire spectrograph images. To our knowledge, other models including both spectral and directional fundus reflectance, are not available. For a more detailed comparison with literature, intersections of the data set were analyzed: spectra at the pupil position with the highest reflectance at 540 nm, and profiles at 540 nm.

B. Mean Spectrum

In Fig. 13B, the mean spectrum (solid line) is compared with literature data. Differences between the spectra depend on (at least) three factors: composition of the population, size of the illuminated and sampled retinal field, and configuration of entrance and exit pupil. The large differences between subjects are very apparent from Fig. 13A, with largest variation below 500 nm.

There is a strong influence of age on the spectra, as absorption in the crystalline lens increases with age.[35] Delori and Pflibsen measured subjects aged 22–38 years.[15] The lack of older subjects may explain the somewhat higher reflectance below 500 nm.

Above 600 nm, a strong dependence on illuminated field size is expected. At the longest wavelengths, where blood does not absorb, light scatters laterally in the deeper fundus layers.[2] Hence, the larger the illuminated field size, the larger reflectance. Delori and Pflibsen illuminated 5 degrees and sampled 1.2–1.6 degrees.[15] Van de Kraats *et al.*[2] illuminated 1.9 and sampled 1.6 degrees. In the present study field sizes were 2.8 and 1.9 degrees. As is seen in Fig. 13B above 600 nm, the reflectance slightly raises with the increment from 1.9 to 2.8 degrees, while the leap to 5 degrees substantially increases reflectance in the red. Below 500 nm, field sizes also influence the spectra. Macular pigment is highly concentrated towards the center of the fovea.[18,36-38] The slightly larger sampled retinal field in the present study reduces macular pigment content and gives rise to higher reflectance in the blue part of the spectrum.

The agreement in the range 520–590 nm is rather remarkable. The present mean spectrum was selected at the Stiles–Crawford maximum. The corresponding pupil plane configuration is similar to the one used by van de Kraats *et al.*[2]: small, closely separated entrance and exit pupils. Both are sensitive for directional reflection and spectra are equally high. Delori and Pflibsen[15] used a modified Zeiss fundus camera, which uses a rather large annular entrance pupil and a concentric circular exit pupil, and should be less sensitive to the directional light. Modification of this arrangement was not reported. It is therefore unclear why the latter spectrum is as high as the other two. Perhaps there is a difference in the absolute calibration of the spectra.

Below 630 nm, mean relative errors RE in Table 1 are smaller than obtained by van de Kraats *et al.*[2] The errors are larger at longer wavelengths. Van de Kraats *et al.*[2] included both instrumental errors and errors due to instability of the subject. In this study integration time was short, largely eliminating errors due to movement of the subject. The errors are largest below 430 nm, where the output of the lamp drops and reflectance is low, and above 730 nm, where the spectral filters block almost all deep-red and infrared light.

C. Spectral Model Results

The results of the spectral model fit are given in Table 2A. Parameters are discussed as in the Table, upwards from the sclera. Deep scatter loss D_{scat} was 0.20, slightly less than 0.23 found by van de Kraats *et al.*[2] The mean thickness of the blood layer Th_{blood} was 68 μm. Van de Kraats *et al.* found 22.7 μm,[2] Delori and Pflibsen 168 μm.[15] Delori and Pflibsen used a model with a Kubelka-Munk scattering description of the deeper layers.[15] This increased the estimated blood layer thickness. Melanin density D_{mela} (1.1 at 500 nm, range 0.95–1.4) is comparable to the densities found by Van de Kraats *et al.* (1.32 at 500 nm, 0.98–1.68).[2] Delori and Pflibsen found a higher mean and a much larger range (2.13 at 500 nm, 0.19–7.9).[15] The former two studies contained only Caucasians, the latter included two Blacks with 3–4 times higher melanin content. This probably explains the differences at the high end of the range.

Receptor disc reflectance R_{disc} cannot be discerned from a reflecting layer at the level of the retinal pigment ephithelium (RPE) in a single bleached spectrum at the Stiles–Crawford maximum. The arguments for attributing reflectance at this level in the retina to the discs in the receptor outer segments are given by van de Kraats *et al.*[2] Mean disc reflectance was 2.8 %, similar to van de Kraats *et al.*, who found 2.75 %.[2] The results can also be compared with RPE reflectance of 2.3 % in the model by Delori and Pflibsen.[15]

The high mean disc reflectance demonstrates the effectiveness of alignment with the Stiles–Crawford maximum. Mean macular pigment density D_{mac} was 0.45 at 460 nm, range 0.28–0.64. Van de Kraats *et al.* found higher values (0.54 at 460 nm, 0.42–0.83).[2] As stated before, this was caused by sampling a smaller retinal field. Delori and Pflibsen found lower values (0.21 at 460 nm, 0.12–0.31).[15] In a more recent paper, Delori *et al.* reported 0.23 for a reflectometric method (sampled field: 2 degrees).[39] With a method based on the autofluorescence of lipofuscin, a fluorophore posterior to the macular pigment, they found 0.48 (sampled field: 2 degrees).[39] The cause for the low reflectometric values may reside in their model, since it lacks reflectors anterior to the macular pigment, e.g., inner limiting membrane and cornea. Accounting for light reflected posterior to the macular pigment gives a higher macular pigment level. Berendschot *et al.* studied the effect of lutein supplementation on D_{mac} in 8 male subjects with a reflectometer and a scanning laser ophthalmoscope (SLO).[8] At baseline, mean D_{mac} was 0.47 for the reflectometric, and 0.26 for the SLO technique.

Reflectance from the inner limiting membrane R_{ilm} is very small and problematic to fit. In many cases the parameter reached the lowest allowed value of zero. Mean R_{ilm} was 0.034 %, even the maximum 0.20 % is lower than the mean R_{ilm} of 0.26 % found by van de Kraats *et al.*[2] They also included data from dark-adapted spectra in the model fit. Undoubtedly, this allowed a better estimate of R_{ilm}. The mean age dependent lens density $D_{lens\text{-}a}$, added with an age independent density 0.31, gives a mean lens density of 0.42 at 420 nm, range 0.31 to 0.79. For some of the young subjects $D_{lens\text{-}a}$ reached the lowest allowed value of zero. As expected, $D_{lens\text{-}a}$ showed a trend with age (data not shown). Van de Kraats *et al.* found a lens density 0.54 at 420 nm, range 0.42 to 0.83, for subjects aged 20 to 51 years, 32 on average.[2] Delori and Pflibsen found a lens density 0.66 for a group of 10 subjects aged 22 to 38 years, mean unknown.[15] The latter result is fairly high given the age of the subjects. The

aging algorithm by Pokorny *et al.* predicts a total lens density at 420 nm of 0.66 at age 22, 0.73 at age 32, and 0.89 at age 50.[35] Compared with these values, reflectometric methods produce systematically low values. Reflectance from the cornea R_{cornea} was on average 0.043 %. This is low in absolute sense, but is of equal magnitude as light reflected from the fundus at wavelengths below 500 nm, especially in older subjects, e.g., see Fig 13A.

The mean confidence interval CI states how accurately parameters are determined in the model fit. A large confidence interval indicates large measurement errors or bad convergence of the fit. For most parameters, except R_{ilm} and R_{cornea}, CI was smaller than σ_N and the range P_{MIN} to P_{MAX}. Apparently, in some cases R_{ilm} and R_{cornea} did not strongly contribute to reflectance and were attributed a very large error. The weakness of the current model is that sometimes parameters are optimized in the fit while being insignificant, or that parameters reach the lower (physical) limit set to zero.

The coefficient of repeatability derived from the total standard deviation CR_T contains the total experimental error. CR_T was smaller or hardly larger than σ_N and well smaller than the range P_{MIN} to P_{MAX}. This means the measurements discriminate well between subjects. CR_T is much larger than CI for D_{mac} and R_{disc}. This indicates that the uncertainty in D_{mac} and R_{disc} results mainly from experimental errors. A high within series CR_S points to errors in fixation and movements of the subject. Between series CR_M is mainly connected to errors in the alignment procedure. For R_{disc} CR_M is largest, most variation is due to variation in alignment on the optical Stiles–Crawford maximum. For D_{mac} CR_S is largest. Macular pigment is highly concentrated towards the center of the fovea.[18,36-38] This makes D_{mac} very sensitive to errors in fixation. The influence of fixation was illustrated in the scatter plot in Fig. 14A. Experienced subjects showed low variability, for some inexperienced subjects (e.g., 9 and 19) variability was large. Fig. 14B demonstrates that

variability in melanin is similar for all subjects. The distribution of melanin pigmentation near the fovea is much smoother than for macular pigment.[18] Therefore, melanin will not be influenced as strongly by fixation errors as macular pigment. With further automation of the set-up and optimization of the protocol, an improvement in the assessment of macular pigment might be expected. It is crucial to observe fixation just before each measurement. Coefficients of repeatability for macular pigment, achieved by Berendschot *et al.*, were 0.27 for a reflectometric technique, and 0.17 with an SLO based technique.[8] Despite the problem with fixation, the present coefficient of repeatability 0.084 was better.

D. Stiles–Crawford Profiles

Profiles at 540 nm clearly showed the optical Stiles–Crawford effect. The profiles were fitted with the commonly used Gaussian model (Eq. 5); results are given in Table 2B. The results are discussed in relation to three earlier studies. (1) Gorrand and Delori scanned the pupil plane with a small exit- and entrance pupil configuration.[25] A 3 degrees retinal field was illuminated with 543 nm HeNe light, the central 2 degrees were sampled. (2) Burns *et al.* used a small entrance pupil and imaged the entire pupil plane on a CCD camera.[26] A series of images was obtained for several entrance pupil positions. The image with highest directional reflectance was selected afterwards. A 2 degrees retinal field was illuminated with 543 nm HeNe light, the central 1 degrees were sampled. (3) De Lint *et al.* used an SLO with a small entrance and exit pupil configuration.[27] The horizontal meridian of the pupil plane is scanned with both pupils, meanwhile obtaining retinal images in 514 nm Argon light. The series of images show the optical Stiles–Crawford effect versus location on the retina. The difference in wavelength with the other studies is considered of minor influence.

In the present study mean x_C was 0.43 ± 0.63 mm nasal (given are PM ± σ_N). Gorrand and Delori reported 0.86 ± 0.84 mm nasal,[25] de Lint *et al.* 0.23 ± 0.41 mm nasal.[27] In the scatter plot of x_C given by Burns *et al.*, the trend to the nasal side is also present.[26] The slight tendency towards the nasal side is common to all studies. Our mean peakedness ρ was 0.17 ± 0.037 mm^{-2}. When compared to the results by Burns *et al.*,[26] 0.0813 ± 0.013 mm^{-2}, this is on the high side. The higher ρ may result from the larger field size (1.9 versus 1.0 degrees), since for small angles ρ increases with eccentricity.[27] Gorrand and Delori,[25] and de Lint *et al.*[27] use a double scanning method which results in a higher ρ: 0.204 ± 0.035 mm^{-2}, and 0.226 ± 0.049 mm^{-2} for the central 2 × 2 degrees of the SLO images. For a more detailed discussion on the differences in ρ between the different techniques, see Marcos and Burns,[40] and Berendschot *et al.*[41] Mean ratio *A/B* of directional light *A* over the non-directional background *B* was 1.5 ± 0.46. This is lower than for Gorrand & Delori, who reported 2.59 ± 0.82,[25] and by de Lint *et al.*, who found 4.9 ± 1.8.[27] The latter authors used a small aperture confocal to the SLO spot on the retina, which strongly suppresses the diffuse background component present with larger fields. With a 1.3 degrees confocal aperture their mean *A/B* decreased to 3.0. Interpretation of CI, CR_T, CR_S and CR_M was discussed previously in Section 5C. The confidence intervals CI are very small compared to the natural variation. The experimental errors CR_T are much larger. Discrimination between subjects was reasonably well. For directional reflectance *A*, CR_M is much larger than CR_S. Variation in *A* mainly originates from alignment on the optical SCE maximum, similar to R_{disc} (see Section 5C).

Simultaneous measurement of spectral and directional reflectance according to the present invention with a simple chin and head-rest proved possible. A video observation channel, and a fast method for optimization of the optical Stiles–Crawford effect at 540 nm allowed alignment with respect to the apparatus and on the Stiles–Crawford maximum within a few minutes.

Application of a short integration time reduced errors due to movement of the subject. Spectral analysis provided densities of photo-stable ocular absorbers such as macular pigment, lens, and melanin and reflectivity of the discs in the outer segment of the cone-receptor cells. Analysis of spatial profiles delivered Stiles–Crawford parameters. Use of all data, not just one spectrum, awaits extension of the fundus reflectance model. Errors in fixation were found to be the main source of within subject variation in macular pigment density. This might be avoided by checking fixation just prior to the measurement. The new apparatus provides a novel diagnostic tool. It might also greatly facilitate epidemiological studies of ocular pigments.

References

1. R. W. Knighton, "Quantitative reflectometry of the ocular fundus," IEEE engineering in medicine and biology **14**, 43-51 (1995).
2. J. van de Kraats, T. T. J. M. Berendschot, and D. van Norren, "The pathways of light measured in fundus reflectometry," Vision Res. **36**, 2229-2247 (1996).
3. A. T. A. Liem, J. E. E. Keunen, and D. van Norren, "*Clinical applications of* fundus reflection densitometry," Surv. Ophthalmol. **41**, 37-50 (1996).
4. D. M. Snodderly, "Evidence for protection against age-related macular degeneration by carotenoids and antioxidant vitamins," Am. J. Clin. Nutr. **62**, 1448S-1461S (1995).
5. J. T. Landrum, R. A. Bone, and M. D. Kilburn, "The macular pigment: a possible role in protection from age-related macular degeneration," Adv. Pharmacol. **38**, 537-556 (1997).
6. S. Beatty, M. Boulton, D. Henson, H. H. Koh, and I. J. Murray, "Macular pigment and age related macular degeneration," Br. J. Ophthalmol. **83**, 867-877 (1999).
7. J. T. Landrum, R. A. Bone, H. Joa, M. D. Kilburn, L. L. Moore, and K. E. Sprague, "A one year study of the macular pigment: the effect of 140 days of a lutein supplement," Exp. Eye Res. **65**, 57-62 (1997).
8. T. T. J. M. Berendschot, R. A. Goldbohm, W. A. A. Klöpping, J. van de Kraats, J. van Norel, and D. van Norren, "Influence of lutein supplementation on macular pigment, assessed with two objective techniques," Invest. Ophthalmol. Vis. Sci. **41**, 3322-3326 (2000).
9. B. R. Hammond, Jr., E. J. Johnson, R. M. Russell, N. I. Krinsky, K. J. Yeum, R. B. Edwards, and D. M. Snodderly, "Dietary modification of human macular pigment density," Invest. Ophthalmol. Vis. Sci. **38**, 1795-1801 (1997).
10. P. J. Delint, T. T. J. M. Berendschot, and D. van Norren, "A comparison of the optical Stiles-Crawford effect and retinal densitometry in a clinical setting," Invest. Ophthalmol. Vis. Sci. **39**, 1519-1523 (1998).
11. P. J. Delint, J. E. Keunen, A. T. Liem, and D. van Norren, "Scanning laser densitometry in visual acuity loss of unknown origin," Br. J. Ophthalmol. **80**, 1051-1054 (1996).
12. C. W. T. A. Lardenoye, K. Probst, P. J. Delint, and A. Rothova, "Photoreceptor function in eyes with macular edema," Invest Ophthalmol Vis Sci **41**, 4048-4053 (2000).
13. D. van Norren and L. F. Tiemeijer, "Spectral reflectance of the human eye," Vision Res. **26**, 313-320 (1986).
14. D. van Norren and J. van de Kraats, "A continuously recording retinal densitometer," Vision Res. **21**, 897-905 (1981).
15. F. C. Delori and K. P. Pflibsen, "Spectral reflectance of the human ocular fundus," Appl. Opt. **28**, 1061-1077 (1989).
16. F. C. Delori, "Spectrophotometer for noninvasive measurement of intrinsic fluorescence and reflectance of the ocular fundus," Appl. Opt. **33**, 7439-7452 (1994).

17. P. E. Kilbride, J. S. Read, G. A. Fishman, and M. Fishman, "Determination of human cone pigment density difference spectra in spatially resolved regions of the fovea," Vision Res. **23**, 1341-1350 (1983).
18. P. E. Kilbride, K. R. Alexander, M. Fishman, and G. A. Fishman, "Human macular pigment assessed by imaging fundus reflectometry," Vision Res. **29**, 663-674 (1989).
19. M. Hammer, D. Schweitzer, L. Leistritz, M. Scibor, K.-H. Donnerhacke, and J. Strobel, "Imaging spectroscopy of the human ocular fundus in vivo," Journal of Biomedical Optics **2**, 418-425 (1997).
20. W. S. Stiles and B. H. Crawford, "The luminous efficiency of rays entering the eye pupil at different points," Proc. R. Soc. Lond. [Biol]. **112**, 428-450 (1933).
21. J. Krauskopf, "Some experiments with a photoelectric ophthalmoscope," in *Performance of the Eye at Low Luminances*, M. A. Bouman and J. J. Vos, eds. (Delft, 1965), pp. 171-181.
22. J. M. Gorrand, "Directional effects of the retina appearing in the aerial image," J. Optics **16**, 279-287 (1985).
23. G. J. van Blokland and D. van Norren, "Intensity and polarization of the light scattered at small angles from the human fovea," Vision Res. **26**, 485-494 (1986).
24. G. J. van Blokland, "Directionality and alignment of the foveal receptors, assessed with light scattered from the human fundus in vivo," Vision Res. **26**, 495-500 (1986).
25. J. M. Gorrand and F. C. Delori, "A reflectometric technique for assessing photoreceptor alignment," Vision Res. **35**, 999-1010 (1995).
26. S. A. Burns, S. Wu, F. C. Delori, and A. E. Elsner, "Direct measurement of human-cone-photoreceptor alignment," J. Opt. Soc. Am. A **12**, 2329-2338 (1995).
27. P. J. Delint, T. T. J. M. Berendschot, and D. van Norren, "Local photoreceptor alignment measured with a scanning laser ophthalmoscope," Vision Res. **37**, 243-248 (1997).
28. D. van Norren and J. van de Kraats, "Imaging retinal densitometry with a confocal Scanning Laser Ophthalmoscope," Vision Res. **29**, 1825-1830 (1989).
29. D. van Norren and J. van de Kraats, "Retinal densitometer with the size of a fundus camera," Vision Res. **29**, 369-374 (1989).
30. G. Wyszecki and W. S. Stiles, *Color Science: Concepts and Methods, Quantitative Data and Formulae* (John Wiley & Sons, 1982).
31. D. R. Lide, *CRC Handbook of Chemistry and Physics* (CRC Press, 1996).
32. G. S. Brindley and E. N. Willmer, "The reflexion of light from the macular and peripheral fundus oculi in man," J. Physiol. **116**, 350-356 (1952).
33. W. H. Press, B. P. Flannery, S. A. Teukolsky, and W. T. Vetterling, *Numerical Recipes in Pascal* (Cambridge University Press, 1989).
34. S. Chinn, "The assessment of methods of measurement," Stat. Med. **9**, 351-362 (1990).
35. J. Pokorny, V. C. Smith, and M. Lutze, "Aging of the human lens," Appl. Opt. **26**, 1437-1440 (1987).
36. D. M. Snodderly, P. K. Brown, F. C. Delori, and J. D. Auran, "The macular pigment. I. Absorbance spectra, localization, and discrimination from other yellow pigments in primate retinas," Invest. Ophthalmol. Vis. Sci. **25**, 660-673 (1984).

37. D. M. Snodderly, J. D. Auran, and F. C. Delori, "The macular pigment. II. Spatial distribution in primate retinas," Invest. Ophthalmol. Vis. Sci. **25**, 674-685 (1984).

38. B. R. Hammond, Jr., B. R. Wooten, and D. M. Snodderly, "Individual variations in the spatial profile of human macular pigment," J. Opt. Soc. Am. A **14**, 1187-1196 (1997).

39. F. C. Delori, D. G. Goger, B. R. Hammond, D. M. Snodderly, and S. A. Burns, "Macular pigment density measured by autofluorescence spectrometry: comparison with reflectometry and heterochromatic flicker photometry," J. Opt. Soc. Am. A **18**, 1212-1230 (2001).

40. S. Marcos and S. A. Burns, "Cone spacing and waveguide properties from cone directionality measurements," J. Opt. Soc. Am. A **16**, 995-1004 (1999).

41. T. T. J. M. Berendschot, J. van de Kraats, and D. van Norren, "Wavelength dependence of the Stiles–Crawford effect explained by perception of backscattered light from the choroid," J. Opt. Soc. Am. A **18**, 1445-1451 (2001).

Table 1. Spectral reflectance data

λ (nm)	*R* (%)	SD	RE (%)	λ (nm)	*R* (%)	SD	RE (%)
420	0.115	0.39	17	590	1.62	0.16	1.0
430	0.162	0.44	5.7	600	2.08	0.17	1.0
440	0.207	0.45	3.4	610	2.31	0.17	1.1
450	0.210	0.45	2.8	620	2.59	0.18	1.1
460	0.219	0.44	2.2	630	2.81	0.18	1.8
470	0.262	0.43	1.8	640	3.05	0.18	2.0
480	0.294	0.41	1.4	650	3.28	0.18	2.2
490	0.332	0.39	1.3	660	3.53	0.18	2.3
500	0.476	0.34	1.1	670	3.77	0.18	1.6
510	0.742	0.28	0.85	680	4.01	0.18	2.2
520	1.04	0.25	0.75	690	4.26	0.17	1.5
530	1.21	0.24	0.68	700	4.47	0.17	2.2
540	1.29	0.23	0.65	710	4.61	0.17	2.5
550	1.33	0.21	0.56	720	4.69	0.16	3.1
560	1.37	0.20	0.68	730	4.71	0.17	4.0
570	1.39	0.19	0.77	740	4.64	0.16	5.8
580	1.42	0.18	0.94	750	4.53	0.16	9.0

λ: wavelength; *R*: mean reflectance; SD: relative between subjects standard deviation, i.e., the standard deviation of the subject means divided by the mean; RE: relative error.

Table 2. Spectral model and Stiles–Crawford parameters

	Parameter	PM	σ_N	P_{MIN}	P_{MAX}	CI	CR_T	CR_S	CR_M
A.	D_{scat}	0.20	0.041	0.11	0.27	0.0066	0.014	0.010	0.010
	Th_{blood} (μm)	68	18	29	104	6.5	15	12	10
	D_{mela}	1.1	0.11	0.95	1.4	0.022	0.045	0.033	0.032
	R_{disc} (%)	2.8	0.50	1.6	3.5	0.050	0.54	0.30	0.47
	D_{mac}	0.45	0.11	0.28	0.64	0.010	0.084	0.071	0.047
	R_{ilm} (%)	0.034	0.052	0	0.20	8.6	0.049	0.039	0.029
	$D_{lens\text{-}a}$	0.11	0.12	0	0.48	0.032	0.058	0.043	0.039
	R_{cornea} (%)	0.043	0.028	0	0.10	4.5	0.029	0.024	0.017
B.	x_C (mm)	0.43^N	0.63	1.3^N	1.3^T	0.0063	0.20	0.13	0.16
	ρ (mm^{-2})	0.17	0.037	0.12	0.23	0.0037	0.036	0.024	0.028
	A (%)	0.77	0.25	0.30	1.14	0.0060	0.22	0.10	0.20
	B (%)	0.52	0.080	0.35	0.65	0.0058	0.084	0.062	0.059
	A/B	1.5	0.46	0.70	2.4	0.026	0.52	0.29	0.45

(A) Spectral model, and (B) Stiles–Crawford parameters. PM: parameter mean; σ_N: between subjects standard deviation; P_{MIN}, P_{MAX}: lowest and highest within subject mean; CI: mean of confidence interval estimations; CR_T, CR_S, CR_M: coefficients of repeatability for the total, within series or between series standard deviation. N and T stand for nasal and temporal.

Claims

1. Apparatus for measurements of at least two specific characteristics of eyes, comprising a light source, means for transferring light from said light source to an eye and light receptor means for reception of light reflected by said eye, wherein said light source comprises means for providing multi-wavelength light, specifically substantially white light, the light receptor means detecting means comprising at least spectrograph means for analysing said light reflected and preferably a video observation means.

2. Apparatus according to claim 1, wherein said means for transferring light to an eye comprises reflecting means having at least one opening for transferring light form said light source to an eye from a side facing away from said eye, at least the side of said reflecting means facing said eye having a reflecting surface for reflection of light reflected by said eye toward said receptor means.

3. Apparatus according to claim 2, wherein said reflecting means comprises a mirror having at least one opening for passage of light.

4. Apparatus according to any one of claims 1 - 3, wherein the receptor means comprises an optical switch for guiding said reflected light at will either to said observation means for video observation or to said detecting means and spectrograph.

5. Apparatus according to claim 4, wherein said switch comprises a movable mirror.

6. Apparatus according to any one of claims 1 - 5, wherein the spectrograph comprises an electronic camera, especially a CCD-camera.

7. Apparatus according to any one of the preceding claims, wherein at least said spectrograph and said observation means are connected to a computer device, comprising software for analysing data received.

8. Apparatus according to claim 7, wherein said software is intended for assessment of:

- spatial distribution of the fundus reflectance in a pupil plane of an eye;
- assessment of the part of the retina used for fixation; and
- assessment of the spectral fundus reflectance along a line in the pupil plane.

9. Apparatus according to any one of the preceding claims, wherein the optical switch comprises means for selecting an image plane.

10. Apparatus according to claim 9, wherein said means comprises at least one lens, especially a lens insertable between two further lenses for rotation of said plane over approximately 90 degrees.

11. Method for measurements of specific characteristics of eyes, especially spatial distribution of the fundus reflectance in the pupil, the part of the retina used for fixation and the spectral fundus reflectance along a line in the pupil plane, wherein a light having different wavelengths, especially white light is directed into an eye, light reflected by said eye being transmitted to a imaging means for electronic analysis of images provided by said light, including a spectrographic analysis.

12. Method according to claim 11, wherein light from a light source is directed into said eye approximately through the centre of the lens system of said eye, wherein light reflected trough peripheral parts of said lens system of said eye is directed to said imaging means.

13. Method according to claim 11 or 12, wherein the reflectance of said light is calibrated in an absolute spectral sense.

14. Method according to any one of claims 11 - 13, wherein light reflected is directed at will either to a video image system or to a spectrograph.

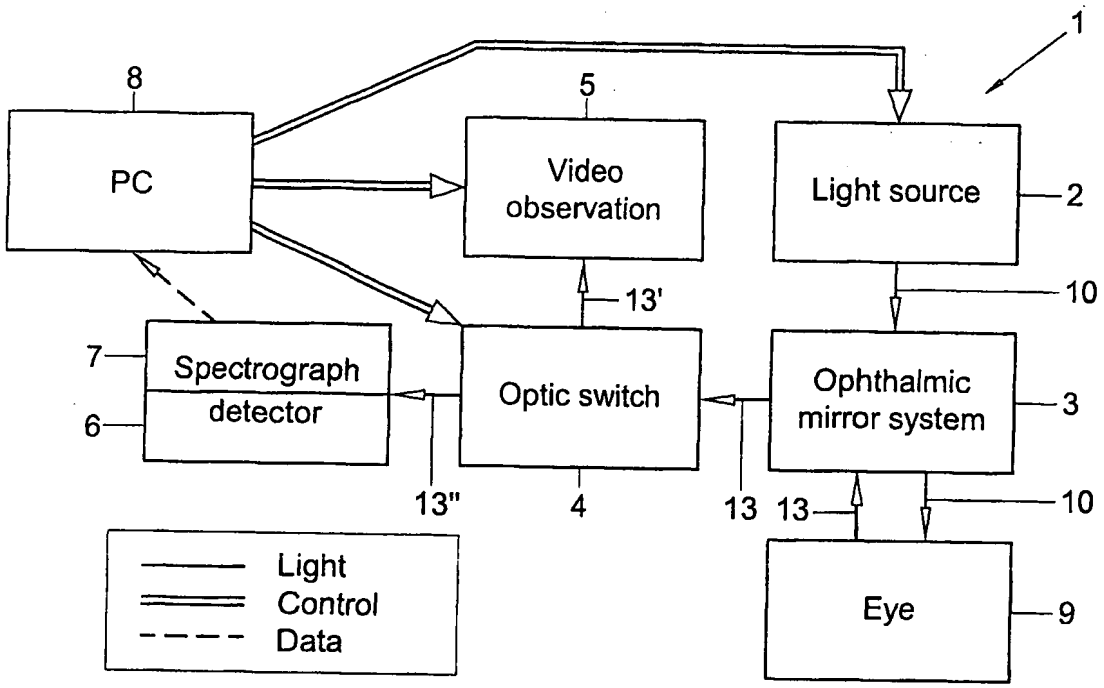

Fig. 1 Schematic representation of the apparatus

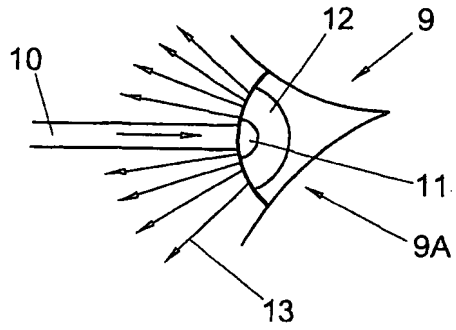

Fig. 1A

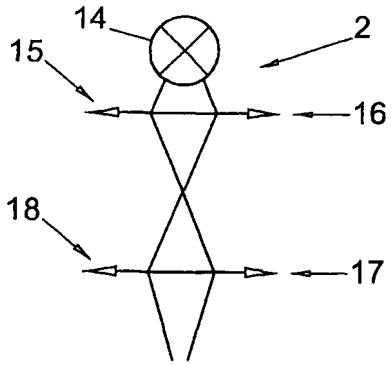

Fig. 2 Light source.

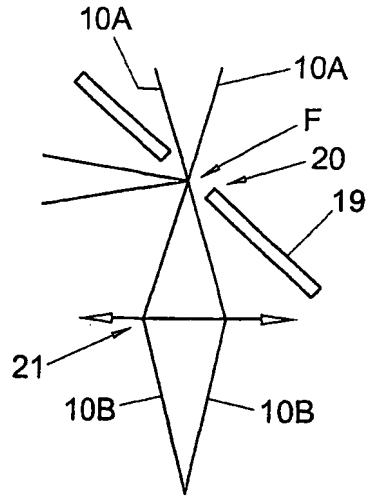

Fig. 3 Ophthalmic mirror system.

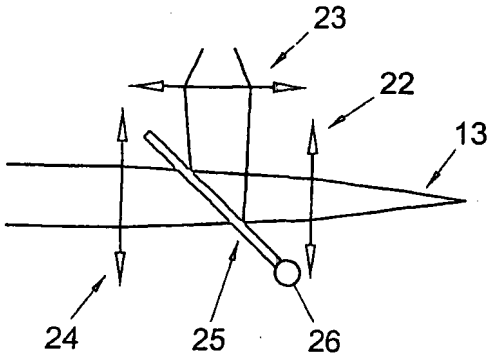

Fig. 4 Optic switch.

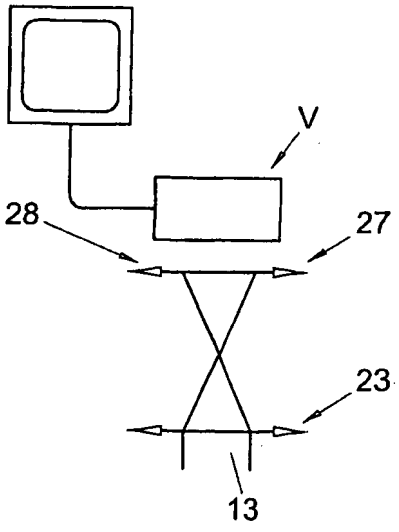

Fig. 5 Video observation

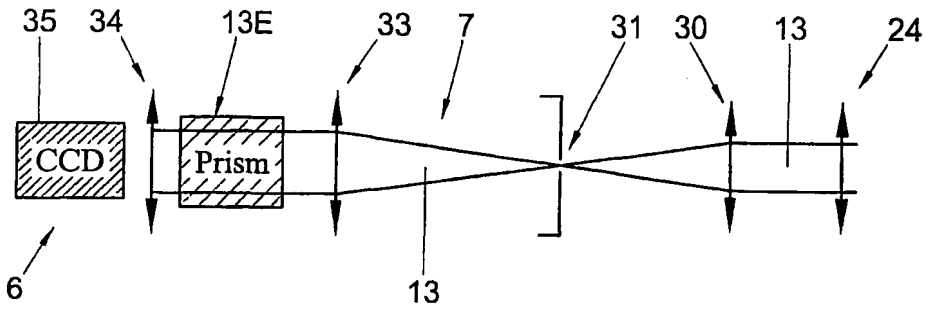

Fig. 6 Spectrograph and detector.

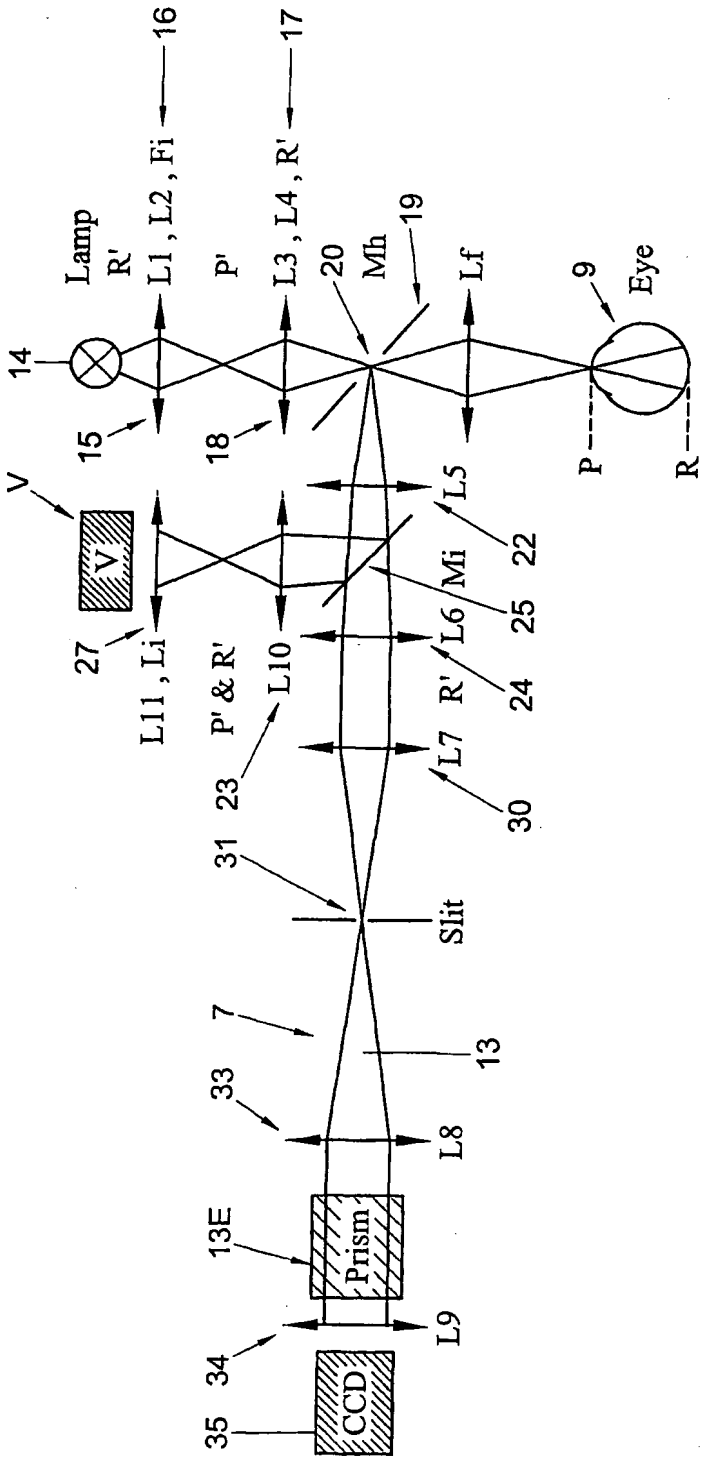

Fig. 7 Schematic of the apparatus; drawing not to scale. P: Pupil plane; R: Retinal plane; P' , R' : Planes conjugate to P, R; Lamp: 30 W halogen lamp; L1 ... L11: Lenses; Fi; Spectral filters; Mh; Mirror with central hole; Lf: Ophthalmic front lens; Mi: Insertable mirror; Li: Insertable lens; V: Video camera; Slit: Slit conjugate to P; Prism: Direct vision prism; CCD: Cooled CCD camera.

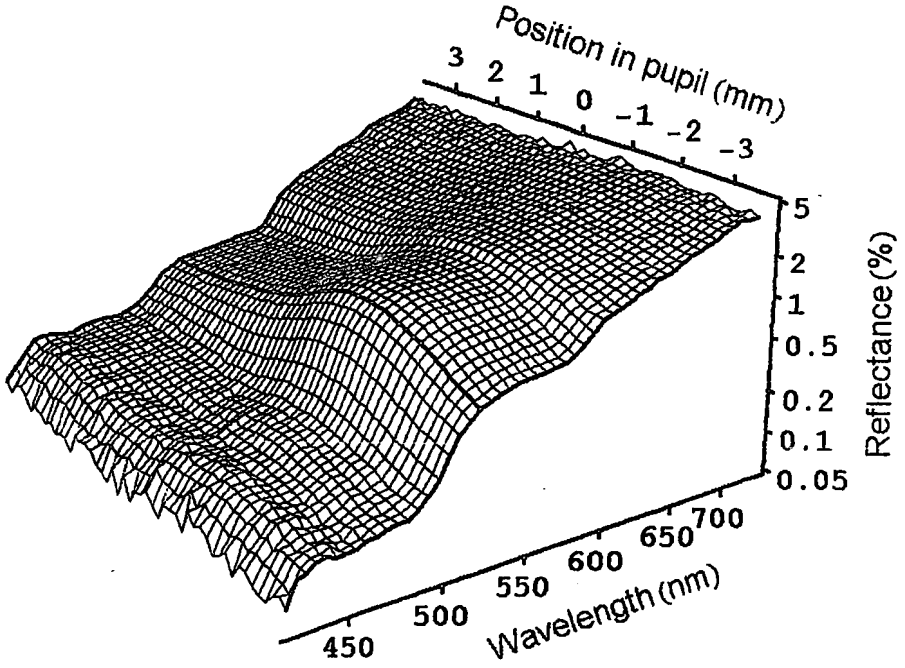

Figure 8. Example of a two-dimensional data-set: percentage reflectance versus wavelength and position in the pupil plane. The data was binned to 5 nm bandwidth in the spectral direction. The common spectral shape of fundus reflectance is recognizable at the borders of the spectrum. As a guide to the eye, a single spatial profile at 525 nm is indicated with the fat line.

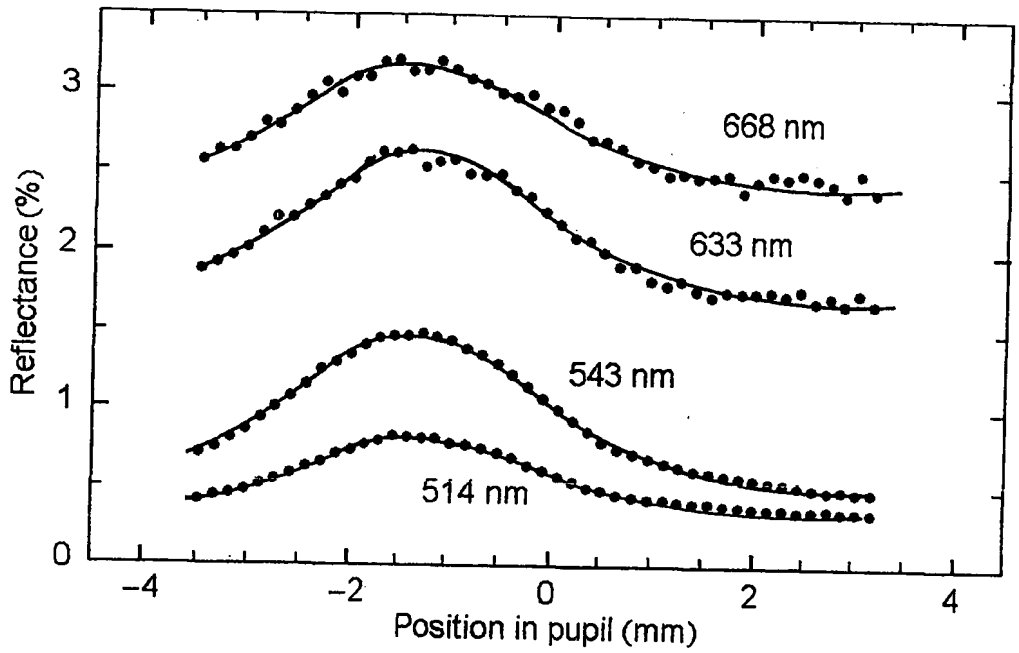

Figure 9. Reflectance versus position in the pupil plane at four different wavelengths. The data is a subset of the data shown in figure 8. The spatial intersections were taken near a number of common laser wavelengths. Data was binned to 5 nm bandwidth before the profiles were obtained. The solid lines are fits of a Gaussian curve to the data.

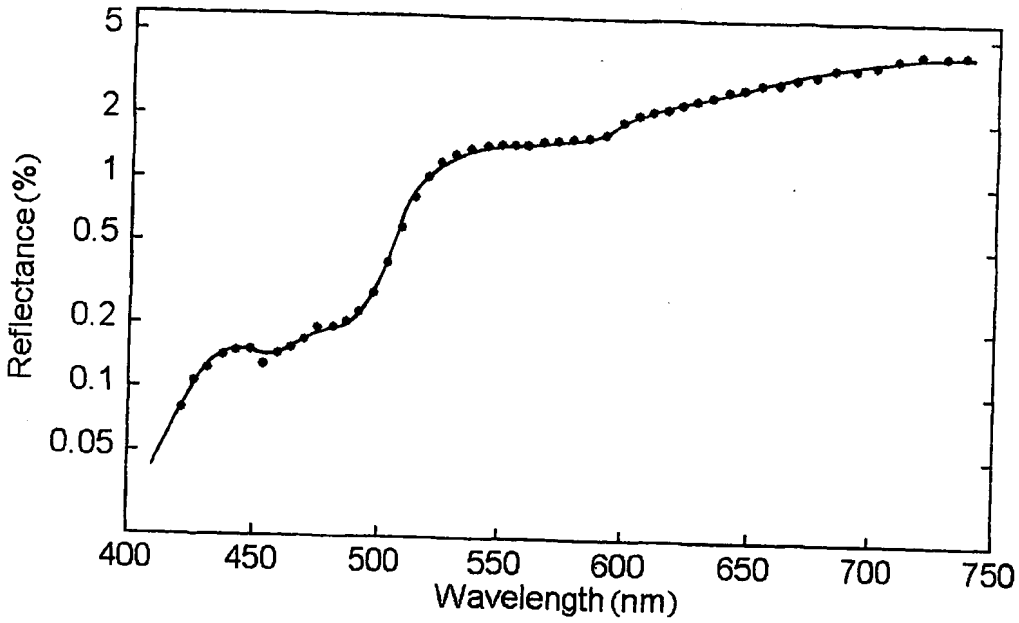

Figure 10. Percentage reflectance versus wavelength. The data is a subset of the data shown in figure 8. The spectral intersection was taken where the spatial intersections show a maximum. The solid line is a model fit to the data.

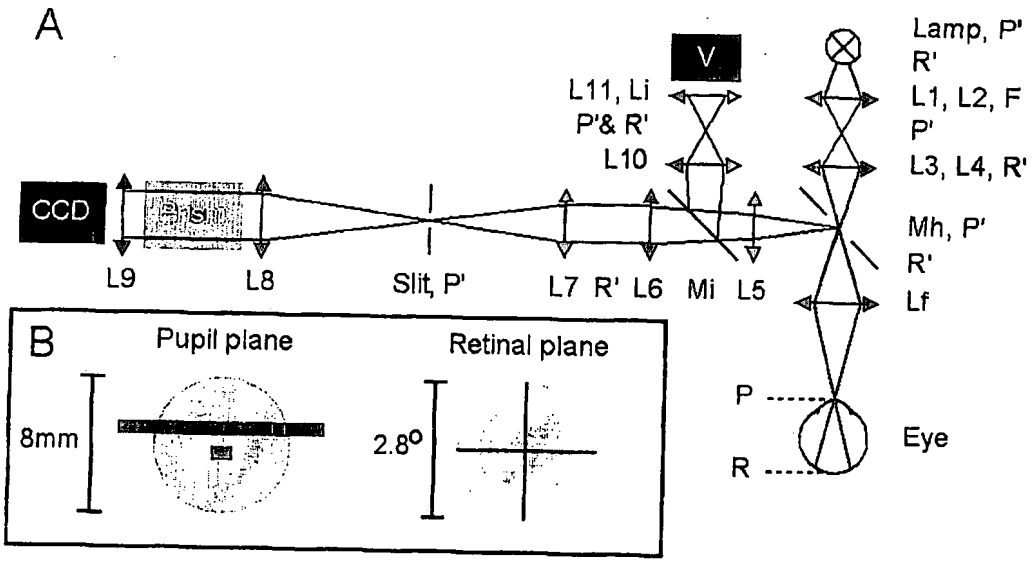

Fig. 11. (**A**) Schematic of the apparatus; drawing not to scale. P: Pupil plane; R: Retinal plane; P', R': Planes conjugate to P, R; Lamp: 30 W halogen lamp; L1 ... L11: Lenses; F: Spectral filters; Mh: Mirror with central hole; Lf: Ophthalmic front-lens; Mi: Insertable mirror; Li: Insertable lens; V: Video camera; Slit: Slit conjugate to P; Prism: Direct vision prism; CCD: Cooled CCD camera. (**B**) Inset: pupil and retinal plane configuration. Left: the disc represents the dilated pupil. The entrance pupil and bar-shaped exit pupil are drawn to scale. Right: the illuminated field, with cross-hairs for fixation, and the concentric sampled field.

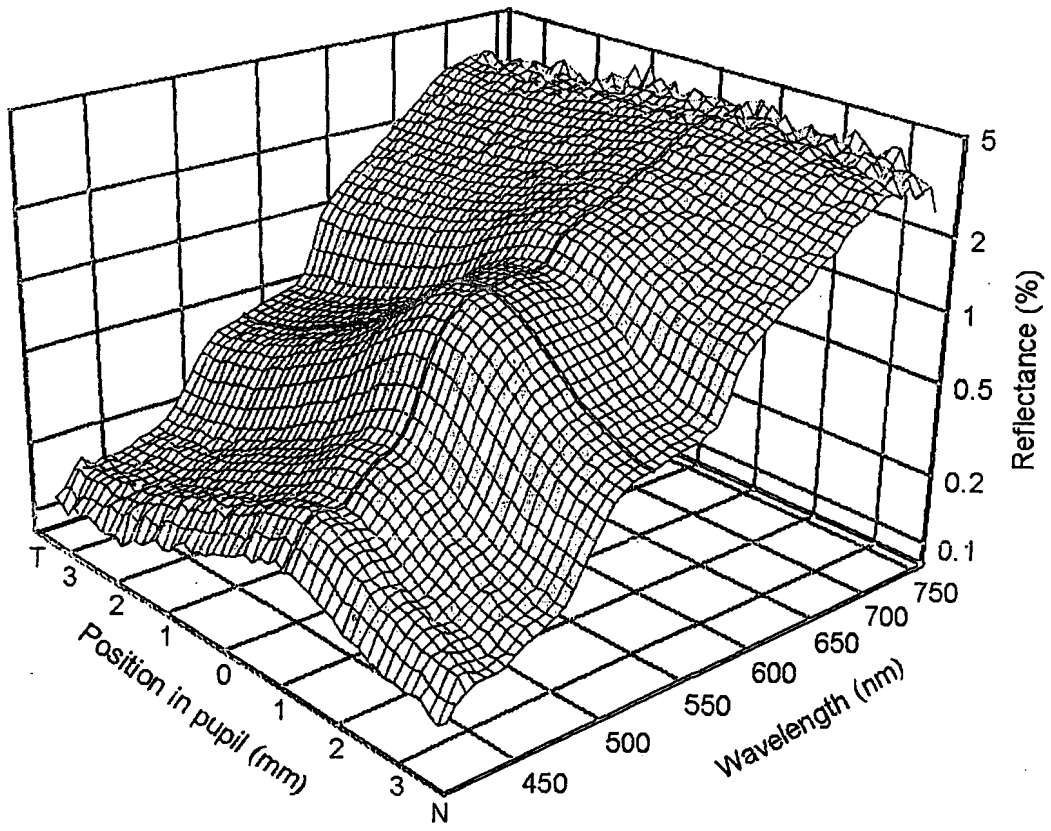

Fig. 12. Image of foveal spectral reflectance (female subject, age 20). Surface height represents equivalent reflectance of the fovea, expressed as a percentage on a logarithmic scale, versus wavelength and position in the pupil plane. Temporal (T) and nasal (N) side are indicated.

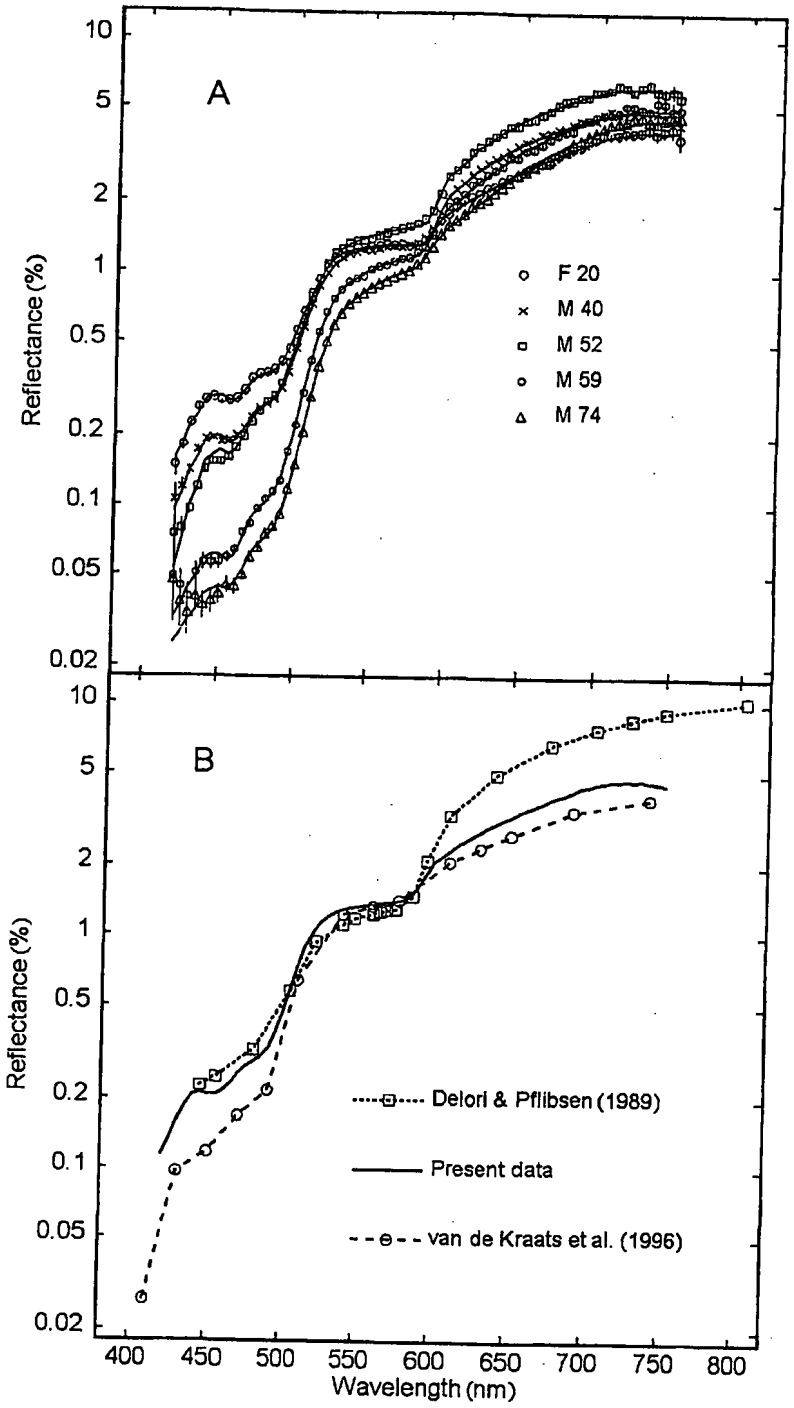

Fig. 13. (A) Spectral intersections, at the pupil position with maximum reflectance at 540 nm. Five subjects spanning the full age-range are presented; gender and age are indicated. Vertical bars indicate the error associated with each point (hardly discernable and absent for most points). The solid lines represent model fits. (B) Mean reflectance spectrum (solid line), together with data from Delori & Pflibsen (1989)[15] and van de Kraats *et al.* (1996).[2] In the mean spectrum, small dips due to macular pigment are present at 460 and 490 nm.

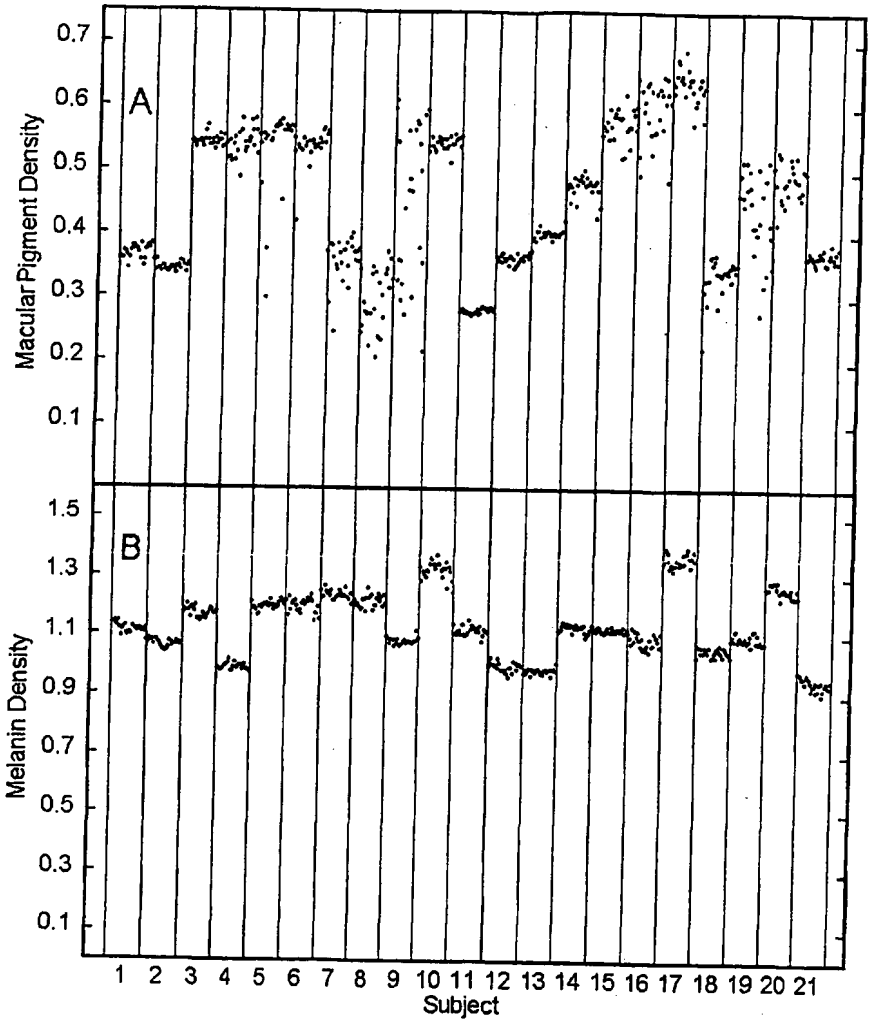

Fig. 14. (A) Macular pigment (D_{mac}), and (B) melanin density (D_{mela}) estimates for all twenty-five measurements per subject. For macular pigment, both between- and within subject variation are large. For melanin they are much smaller. Macular pigment within subject variation is markedly different between subjects; e.g., subject 11 has little variation, whereas in subject 9 the data is highly scattered. The latter subject had difficulties maintaining rigid fixation during alignment.

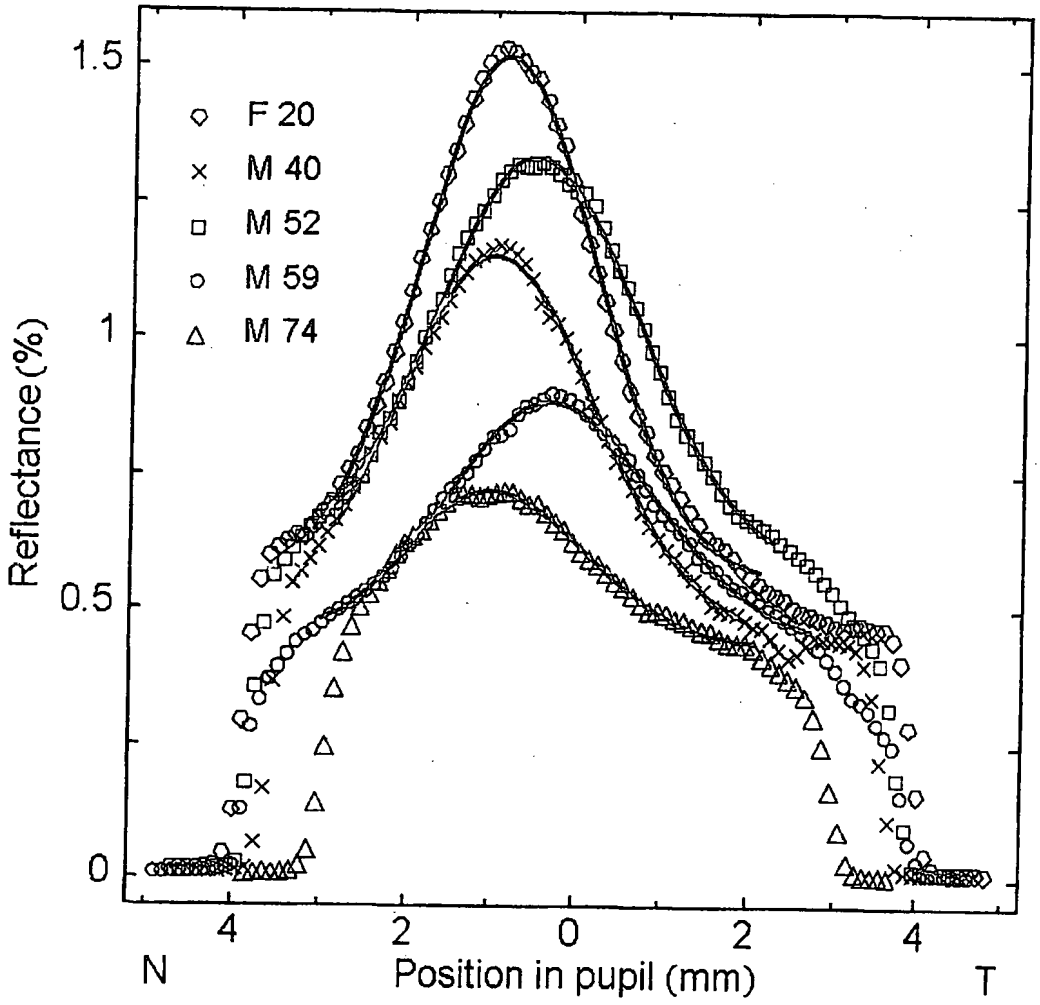

Fig. 15. Profiles at 540 nm demonstrating individual differences in the optical Stiles–Crawford effect. Data is for the same subjects as in Fig. 3; gender and age are given. Solid lines represent fits to the data. Nasal (N) and temporal (T) side are indicated. Pupil edges are recognizable as the sharp drops in the region 3 to 4 mm. Maximum reflectance shows up near the center of the pupil, with a tendency towards the nasal side.

INTERNATIONAL SEARCH REPORT

PCT/NL 02/00290

A. CLASSIFICATION OF SUBJECT MATTER
IPC 7 A61B3/10 A61B3/14

According to International Patent Classification (IPC) or to both national classification and IPC

B. FIELDS SEARCHED

Minimum documentation searched (classification system followed by classification symbols)
IPC 7 A61B

Documentation searched other than minimum documentation to the extent that such documents are included in the fields searched

Electronic data base consulted during the international search (name of data base and, where practical, search terms used)
EPO-Internal, PAJ, WPI Data

C. DOCUMENTS CONSIDERED TO BE RELEVANT

Category °	Citation of document, with indication, where appropriate, of the relevant passages	Relevant to claim No.
X	DE 199 07 479 A (UNIV SCHILLER JENA) 17 August 2000 (2000-08-17) column 3, line 46 -column 4, line 15 figure 1	1-10
X	US 6 149 589 A (DIACONU VASILE ET AL) 21 November 2000 (2000-11-21) column 3, line 62 -column 5, line 57 figure 1	1-10
X	DE 44 10 690 C (UNIV SCHILLER JENA) 29 June 1995 (1995-06-29) column 6, line 62 -column 7, line 27 column 10, line 14 - line 29 figures 1,10	1-10

-/--

[X] Further documents are listed in the continuation of box C.

[X] Patent family members are listed in annex.

° Special categories of cited documents :

"A" document defining the general state of the art which is not considered to be of particular relevance

"E" earlier document but published on or after the international filing date

"L" document which may throw doubts on priority claim(s) or which is cited to establish the publication date of another citation or other special reason (as specified)

"O" document referring to an oral disclosure, use, exhibition or other means

"P" document published prior to the international filing date but later than the priority date claimed

"T" later document published after the international filing date or priority date and not in conflict with the application but cited to understand the principle or theory underlying the invention

"X" document of particular relevance; the claimed invention cannot be considered novel or cannot be considered to involve an inventive step when the document is taken alone

"Y" document of particular relevance; the claimed invention cannot be considered to involve an inventive step when the document is combined with one or more other such documents, such combination being obvious to a person skilled in the art.

"&" document member of the same patent family

Date of the actual completion of the international search	Date of mailing of the international search report
27 September 2002	08/10/2002

Name and mailing address of the ISA	Authorized officer
European Patent Office, P.B. 5818 Patentlaan 2 NL - 2280 HV Rijswijk Tel. (+31-70) 340-2040, Tx. 31 651 epo nl, Fax: (+31-70) 340-3016	Lohmann, S

Form PCT/ISA/210 (second sheet) (July 1992)

INTERNATIONAL SEARCH REPORT

PCT/NL 02/00290

C.(Continuation) DOCUMENTS CONSIDERED TO BE RELEVANT

Category *	Citation of document, with indication, where appropriate, of the relevant passages	Relevant to claim No.
X	HAMMER M ET AL: "IMAGING SPECTROSCOPY OF THE HUMAN OCULAR FUNDUS IN VIVO" JOURNAL OF BIOMEDICAL OPTICS, INTERNATIONAL SOCIETY FOR OPTICAL ENGINEERING (SPIE), US, vol. 2, no. 4, October 1997 (1997-10), pages 418-425, XP001057493 ISSN: 1083-3668 paragraph '02.1!; figure 1 ---	1-10
X	DELORI F C ET AL: "SPECTRAL REFLECTANCE OF THE HUMAN OCULAR FUNDUS" APPLIED OPTICS, OPTICAL SOCIETY OF AMERICA,WASHINGTON, US, vol. 28, no. 6, 15 March 1989 (1989-03-15), pages 1061-1077, XP000029737 ISSN: 0003-6935 paragraph 'II.A!; figure 1 -----	1-10

Form PCT/ISA/210 (continuation of second sheet) (July 1992)

INTERNATIONAL SEARCH REPORT

PCT/NL 02/00290

Box I Observations where certain claims were found unsearchable (Continuation of item 1 of first sheet)

This International Search Report has not been established in respect of certain claims under Article 17(2)(a) for the following reasons:

1. [X] Claims Nos.: 11-14
because they relate to subject matter not required to be searched by this Authority, namely:

Rule 39.1(iv) PCT - Diagnostic method practised on the human or animal body under ultimate supervision of a doctor

2. [ ] Claims Nos.:
because they relate to parts of the International Application that do not comply with the prescribed requirements to such an extent that no meaningful International Search can be carried out, specifically:

3. [ ] Claims Nos.:
because they are dependent claims and are not drafted in accordance with the second and third sentences of Rule 6.4(a).

Box II Observations where unity of invention is lacking (Continuation of item 2 of first sheet)

This International Searching Authority found multiple inventions in this international application, as follows:

1. [ ] As all required additional search fees were timely paid by the applicant, this International Search Report covers all searchable claims.

2. [ ] As all searchable claims could be searched without effort justifying an additional fee, this Authority did not invite payment of any additional fee.

3. [ ] As only some of the required additional search fees were timely paid by the applicant, this International Search Report covers only those claims for which fees were paid, specifically claims Nos.:

4. [ ] No required additional search fees were timely paid by the applicant. Consequently, this International Search Report is restricted to the invention first mentioned in the claims; it is covered by claims Nos.:

Remark on Protest

[ ] The additional search fees were accompanied by the applicant's protest.

[ ] No protest accompanied the payment of additional search fees.

INTERNATIONAL SEARCH REPORT

PCT/NL 02/00290

Patent document cited in search report	Publication date	Patent family member(s)	Publication date
DE 19907479 A	17-08-2000	DE 19907479 A1	17-08-2000
US 6149589 A	21-11-2000	US 5919132 A	06-07-1999
		AU 2918699 A	18-10-1999
		CA 2323434 A1	30-09-1999
		WO 9948418 A1	30-09-1999
		EP 1065968 A1	10-01-2001
		JP 2002507445 T	12-03-2002
DE 4410690 C	29-06-1995	DE 4410690 C1	29-06-1995